*Published online 17 March 2023*

*Nucleic Acids Research, 2023, Vol. 51, No. 14* ***7563–7579***
*https://doi.org/10.1093/nar/gkad139*

# Restoration of mitochondrial function through activation of hypomodified tRNAs with pathogenic mutations associated with mitochondrial diseases

**Ena Tomoda[1], Asuteka Nagao[1,*], Yuki Shirai[1], Kana Asano[1], Takeo Suzuki[1], Brendan J. Battersby[2] and Tsutomu Suzuki[1,*]**

[1]Department of Chemistry and Biotechnology, Graduate School of Engineering, University of Tokyo, 7-3-1 Hongo, Bunkyo-ku, Tokyo 113-8656, Japan and [2]Institute of Biotechnology, University of Helsinki, Helsinki 00790, Finland

Received November 07, 2022; Revised February 14, 2023; Editorial Decision February 15, 2023; Accepted March 08, 2023

## ABSTRACT

**Mutations in mitochondrial (mt-)tRNAs frequently cause mitochondrial dysfunction. Mitochondrial myopathy, encephalopathy, lactic acidosis, and stroke-like episodes (MELAS), and myoclonus epilepsy associated with ragged red fibers (MERRF) are major clinical subgroups of mitochondrial diseases caused by pathogenic point mutations in tRNA genes encoded in mtDNA. We previously reported a severe reduction in the frequency of 5-taurinomethyluridine ($\tau m^5U$) and its 2-thiouridine derivative ($\tau m^5s^2U$) in the anticodons of mutant mt-tRNAs isolated from the cells of patients with MELAS and MERRF, respectively. The hypomodified tRNAs fail to decode cognate codons efficiently, resulting in defective translation of respiratory chain proteins in mitochondria. To restore the mitochondrial activity of MELAS patient cells, we overexpressed *MTO1*, a $\tau m^5U$-modifying enzyme, in patient-derived myoblasts. We used a newly developed primer extension method and showed that *MTO1* overexpression almost completely restored the $\tau m^5U$ modification of the MELAS mutant mt-tRNA$^{Leu(UUR)}$. An increase in mitochondrial protein synthesis and oxygen consumption rate suggested that the mitochondrial function of MELAS patient cells can be activated by restoring the $\tau m^5U$ of the mutant tRNA. In addition, we confirmed that *MTO1* expression restored the $\tau m^5s^2U$ of the mutant mt-tRNA$^{Lys}$ in MERRF patient cells. These findings pave the way for epitranscriptomic therapies for mitochondrial diseases.**

## INTRODUCTION

Mitochondria are eukaryotic organelles that produce most of the cellular energy in the form of ATP through a process referred to as oxidative phosphorylation (OXPHOS). Mitochondria also play a critical role in various physiological activities and metabolic processes, including generation of reactive oxygen species (ROS), intracellular $Ca^{2+}$ homeostasis, heme and steroid biogenesis, regulation of proliferation and differentiation, and programmed cell death (1). Mitochondria have their own genome, called mitochondrial DNA (mtDNA), and its expression system (2). Human mtDNA is a circular double-stranded DNA encoding 37 genes: 13 for the essential subunits of respiratory complexes, 22 for tRNAs (mt-tRNAs), and 2 for rRNAs (mt-rRNAs) (3). To translate 13 proteins, mitochondria have their own protein synthesis machinery, which consists of mitochondrial ribosomes (mitoribosomes), mt-tRNAs, and several translational factors (2,4–6). All RNA components required for the mitochondrial translational apparatus are encoded in mtDNA, whereas its protein components are encoded in the nuclear genome, translated in the cytoplasm, and imported to mitochondria.

Dysregulation of mitochondrial activities has pathological outcomes (1,7,8). Mitochondrial diseases are clinically and genetically heterogeneous disorders caused by mitochondrial dysfunction (7,9). Because efficient mitochondrial activity is particularly necessary for energy-consuming organs such as the brain and muscles, mitochondrial diseases are also called 'mitochondrial encephalomyopathies' (10). Several human diseases are associated with pathogenic mutations in mtDNA and/or nuclear genes responsible for mitochondrial function. Of 997 pathogenic mutations in mtDNA identified to date, 374 are located in mt-tRNA genes (MITOMAP, www.mitomap.org) (11,12), suggesting

*To whom correspondence should be addressed. Tel: +81 70 1535 1488; Email: ts@chembio.t.u-tokyo.ac.jp
Correspondence may also be addressed to Asuteka Nagao. Email: asuteka@chemibo.t.u-tokyo.ac.jp
Present address: Takeo Suzuki, Department of Medical Biochemistry, Graduate School of Medicine, University of the Ryukyus, 207 Uehara, Nishihara, Okinawa 903-0215, Japan.

that pathogenic mutations in mt-tRNAs are particularly associated with mitochondrial diseases.

Mitochondrial myopathy, encephalopathy, lactic acidosis, and stroke-like episodes (MELAS) (13) and myoclonus epilepsy associated with ragged red fibers (MERRF) (14) are major and well-characterized clinical subgroups of mitochondrial diseases caused by point mutations in the mt-tRNA$^{Leu(UUR)}$ (15–17) and mt-tRNA$^{Lys}$ genes (18), respectively. Approximately 80% of individuals with MELAS have an A-to-G point mutation at position 3243 (3243A > G) in the mt-tRNA$^{Leu}$ gene responsible for the UUR codons (Figure 1A), and another 10% have a 3271T > C mutation in the same tRNA gene (Figure 1A). Many individuals with MERRF have an 8344A > G mutation in the mt-tRNA$^{Lys}$ gene (Figure 1B).

The position 3243 in mtDNA corresponds to position 14 in mt-tRNA$^{Leu\ (UUR)}$ (Figure 1A). In the canonical tRNA structure, A14 makes a reverse-Hoogsten base pair with U8 to stabilize the tRNA core region. It has been speculated that the 3243A > G mutation destabilizes the mutant tRNA in MELAS patient cells (19,20). Our group previously reported that the steady-state level and half-life of the 3243A > G mutant tRNA are significantly decreased (21). The aminoacylation level of the mutant tRNA is also reduced to approximately 70% of that of the wild-type tRNA (21).In addition, several studies have shown that the 3243A > G MELAS mutation impairs transcription termination (22), tRNA processing (23), proper tRNA conformation (24), and aminoacylation (25–27), thereby hampering the synthesis of respiratory chain proteins by mitochondria (28,29) and leading to respiratory deficiency (30–32).

The most striking finding in the MELAS mutant tRNA is loss of tRNA modification. We observed severe impairment of 5-taurinomethyluridine ($\tau m^5U$) in mt-tRNA$^{Leu(UUR)}$ isolated from MELAS patient cells with 3243A > G, 3271U > C, or other mutations (3244G > A, 3258U > C and 3291U > C) associated with MELAS (Figure 1A) (21,33). These findings strongly suggest that MELAS mutations hinder recognition by GTPBP3 and MTO1, an enzymatic complex responsible for the $\tau m^5U$ modification (Figure 1C) (34). $\tau m^5U$ is a unique tRNA modification that is specifically present at the first position of the anticodon of the mt-tRNAs for Leu(UUR) and Trp, and its 2-thiouridine derivative, 5-taurinomethyl-2-thiouridine ($\tau m^5s^2U$), is present at the same position in mt-tRNAs for Lys, Gln, and Glu (Figure 1C) (35,36). The hypomodified mt-tRNA$^{Leu(UUR)}$ lacking $\tau m^5U$ normally decodes the UUA codon but fails to decode the UUG codon efficiently (37), indicating that $\tau m^5U$ at position 34 ($\tau m^5U34$) stabilizes U–G wobble pairing at the A site of the ribosome (38). Ribosome profiling revealed that mitoribosomes frequently accumulate at the UUG codon in fibroblasts bearing the 3243A > G mutation as well as in *MTO1*-knockout (KO) cells (39), demonstrating that $\tau m^5U34$ is crucial for UUG decoding in mitochondrial translation. The synthesis of ND6, a mtDNA-encoded subunit of respiratory chain complex I, in mitochondria decreases as the mutation rate of 3243A > G in mtDNA increases (32,40). Because ND6 has the highest usage of UUG codons among the 13 genes encoded in mtDNA, its translation is severely affected by loss of $\tau m^5U$ in the MELAS mutant tRNA. This molecular mechanism explains why complex I deficiency is the major biochemical symptom of MELAS (41,42). We also found loss of $\tau m^5s^2U$ in mt-tRNA$^{Lys}$ with the 8344A > G mutation isolated from MERRF patient cells (Figure 1B) (43–45). The hypomodified mt-tRNA$^{Lys}$ was unable to efficiently decode either AAA or AAG codons, leading to defective mitochondrial translation and respiratory activity (43,46). Partial modification of 1-methyladenosine ($m^1A$) at position 58 is also impaired in the MERRF mutant mt-tRNA$^{Lys}$ (Figure 1B) (47).

The pathogenic mutations associated with MELAS and MERRF prevent $\tau m^5U$-modifying enzymes from recognizing their substrate tRNAs. $\tau m^5U$ formation is catalyzed by MTO1 and GTPBP3 in the presence of taurine and 5,10-methylene-tetrahydrofolate ($CH_2$-THF) as substrates, and GTP, FAD, NADH and $K^+$ as cofactors (Figure 1C) (34). We used a metabolic labeling experiment to demonstrate that the β-carbon of L-serine is a source of the methylene group of $\tau m^5(s^2)U$ via $CH_2$-THF in one-carbon (1C) metabolism. This finding is supported by the observation that the $\tau m^5(s^2)U$ frequency is reduced in cells harboring mutations in *SHMT2* and mitochondrial folate transporter (*MTF*) (34).

The physiological importance of $\tau m^5(s^2)U$ has been demonstrated by pathogenic mutations in *MTO1* and *GTPBP3*. Loss-of-function mutations of these genes are associated with hypertrophic cardiomyopathy and lactic acidosis (48–50). Patients with these mutations exhibit mitochondrial dysfunction characterized by low oxygen consumption and respiratory chain activity. *Mto1* KO mouse embryos die at an early developmental stage, and heart-specific *Mto1* conditional KO mice die within 24 h after birth (51). These observations demonstrate that $\tau m^5U$ is essential for animal development. *Mto1* KO cells are characterized by abnormal mitochondrial protein synthesis and the accumulation of protein aggregates in the cytoplasm, indicating that $\tau m^5U$ contributes to cellular proteostasis (51). Pathogenic mutations in *GTPBP3* are also associated with Leigh syndrome (48), which is a progressive encephalopathy associated with mitochondrial dysfunction, indicating that the physiological roles of GTPBP3 are different from those of MTO1.

Several approaches have been used in the treatment of mitochondrial diseases (52). Recent advances in genetic manipulation technologies of mammalian mtDNA provide new possibilities for the future therapy of mitochondrial diseases (53). Mitochondria-targeting versions of zinc-finger nucleases (mitoZFNs) (54) and transcription activator-like effector nucleases (mitoTALENs) (55) have been applied to eliminate mtDNA with pathogenic mutations. The mitoTALENs successfully eliminate mtDNA with the 3243A > G mutation in MELAS-derived iPS cells (56). In an RNA-focused approach, overexpression of mitochondrial leucyl-tRNA synthetase (LARS2) (57,58) or its C-terminal peptide partially restored mitochondrial function in cybrid cells with 3243A > G mutations (59–62). LARS2, especially its C-terminal domain, may stabilize mt-tRNA with pathogenic mutations, thereby restoring mitochondrial function. In MERRF with the 8344A > G mutation, mitochondrial protein synthesis in MERRF

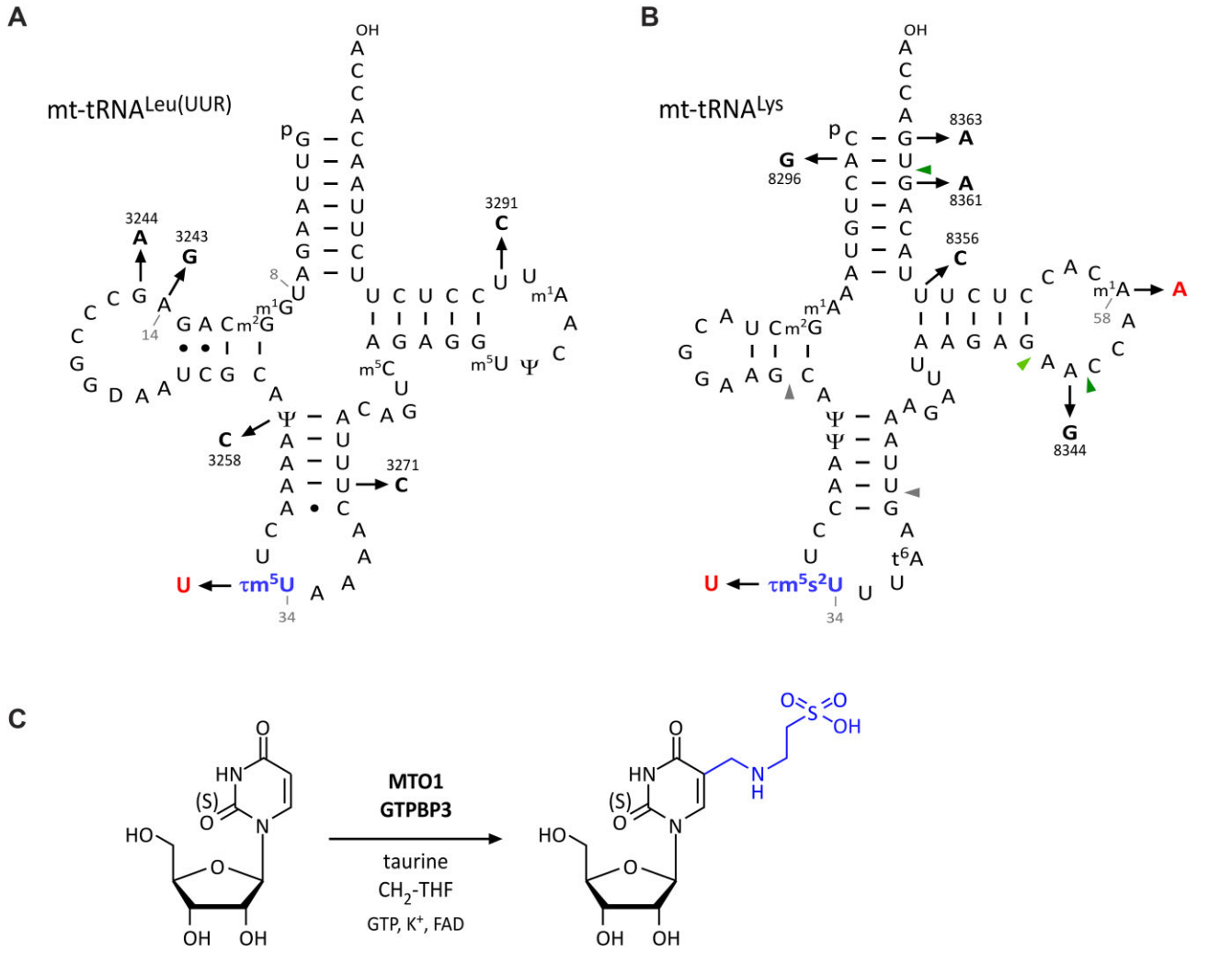


**Figure 1.** $\tau m^5s^2U$ modification of mitochondrial tRNAs and pathogenic mutations. (**A**) Secondary structure of human mt-tRNA$^{Leu(UUR)}$ with post-transcriptional modifications: p, 5′-phosphate; OH, 3′-hydroxy terminus; $m^1G$, 1-methylguanosine; $m^2G$, $N^2$-methylguanosine; Ψ, pseudouridine; $\tau m^5U$, 5-taurinomethyluridine; $m^5C$, 5-methylcytidine; $m^5U$, 5-methyluridine; $m^1A$, 1-methyladenosine. MELAS mutations are numbered according to mtDNA positions. tRNA positions are numbered in gray. (**B**) Secondary structure of human mt-tRNA$^{Lys}$ with post-transcriptional modifications: p, 5′-phosphate; OH, 3′-hydroxy terminus; $m^1A$, 1-methyladenosine; $m^2G$, $N^2$-methylguanosine; Ψ, pseudouridine; $\tau m^5s^2U$, 5-taurinomethyl-2-thiouridine; $t^6A$, $N^6$-threonylcarbamoyladenosine. MERRF mutations are numbered according to mtDNA positions. Gray and green arrowheads indicate the cleavage sites of RNase $T_1$ to generate the anticodon-containing fragment and $m^1A$-containing fragment, respectively. (**C**) Biogenesis of $\tau m^5(s^2)U34$ on mt-tRNA. The 5-taurinomethyl group is shown in blue. $\tau m^5U$ is synthesized by the GTPBP3/MTO1 complex using 5,10-$CH_2$-THF and taurine as substrates, and cofactors including GTP, potassium ion, and FAD.

myoblasts was partially activated by overexpression of *MTO1* or *TRMT61B* (47), a tRNA methyltransferase responsible for 1-methyladenosine ($m^1A$) at position 58 (63), because both $\tau m^5s^2U34$ and $m^1A58$ are impaired in the MERRF mutant mt-tRNA$^{Lys}$. Restoration of $m^1A58$ was confirmed, whereas the status of $\tau m^5s^2U34$ remains to be investigated.

Based on our reports of $\tau m^5U$ deficiency in MELAS patients, high-dose oral taurine supplementation was investigated in Japan as a potential therapy for MELAS (64). An expanded clinical trial showed that taurine supplementation significantly suppressed stroke-like episodes in MELAS patients without any severe adverse events (65). In 2019, high-dose taurine supplementation was officially approved in Japan as a MELAS treatment covered by medical insurance. However, brain atrophy remains progressive after the treatment, suggesting that this method does not lead to a fundamental treatment for MELAS.

The aim of the present study was to restore mitochondrial function in MELAS patient cells through the activation of mutant tRNA. To this end, we overexpressed *MTO1* or *GTPBP3* in MELAS myoblasts and analyzed the $\tau m^5U$ modification status in mt-tRNA$^{Leu(UUR)}$ with the 3243A > G mutation. We first developed a primer extension method (CMC-PE) to accurately quantify the $\tau m^5U$ modification on mt-tRNA$^{Leu(UUR)}$, and found that *MTO1* overexpression almost completely restored the $\tau m^5U$ modification of the MELAS mutant tRNA, whereas overexpression of *GTPBP3* did not. We also found that *MTO1* overexpression significantly increased the *in vivo* aminoacylation

level of the MELAS mutant tRNA. However, the steady-state level of the MELAS mutant tRNA was unchanged even if the $\tau m^5U$ modification was fully introduced. Overexpression of *MTO1* partially but significantly increased mitochondrial protein synthesis and the oxygen consumption rate in MELAS myoblasts. In addition, we confirmed that *MTO1* expression restored $\tau m^5s^2U$ of the mutant mt-tRNA in MERRF patient cells. These findings demonstrate that the mitochondrial function of pathogenic cells can be activated by restoring the taurine modification of hypomodified tRNAs derived from MELAS and MERRF.

## MATERIALS AND METHODS

### Cell culture

HeLa and HEK293T cells were cultured at 37°C in 5% $CO_2$ in Dulbecco's modified Eagle medium (DMEM) (high-glucose) supplemented with 5% fetal bovine serum (FBS) and 1% penicillin–streptomycin (PS). For culturing HeLa cells, the medium was supplemented with 10 mM taurine. *GTPBP3* KO cells were generated previously (34). The MELAS myoblasts were derived from a muscle biopsy specimen taken from a 6 years old female patient who presented with stroke-like episodes and was diagnosed with MELAS (29). Homoplasmic myoblasts for WT or 3243A > G mutation were derived from the same MELAS patient and clonally selected (29). Homoplasmic myoblasts for WT or 8344A > G mutation were derived from satellite cells of MERRF patient and immortalized with E6/E7 and hTERT (46). The MERRF myoblasts transduced by MTO1 or TRMT61B were generated previously (47). The myoblasts were cultured at 37°C in 5% $CO_2$ in Cell Applications Inc. Skeletal Muscle Cell Growth Medium (#151-500, Lonza) supplemented with 0.05 g/l uridine and 10 mM taurine, but GA-1000 was substituted for 1% PS.

### Construction of vectors

A series of vectors were constructed using the SLiCE method (66). Human *MTO1* fused with C-terminal FLAG tag (MTO1-FLAG) and human *GTPBP3* were PCR-amplified from pDEST_MTO1 and pDEST_GTPBP3 (34), respectively, using KOD-Plus-Neo DNA polymerase (TOYOBO Co. Ltd) with a set of primers (Supplementary Table S1). pLenti CMV GFP Puro (658-5) (Addgene #17448) was linearized by PCR with a set of primers (Supplementary Table S1). The PCR products of *MTO1*-FLAG or *GTPBP3* and the linearized vectors were fused by *in vitro* homologous recombination using the SLiCE method to construct pLenti_MTO1_FLAG and pLenti_GTPBP3. To construct the L2CTD-FLAG vector, the MTS of *COX8* was first inserted at the 5′ terminus of the GFP ORF in pLenti CMV GFP Puro (658-5) to construct pLenti-MTSGFP, which was then linearized by PCR with a set of primers (Supplementary Table S1). The cDNA of human *LARS2* without its MTS (MASVWQRLGFYASLLKRQ) was amplified from HeLa total RNA as a template by RT-PCR with a set of primers (Supplementary Table S1), and cloned into pET-21b (Novagen) at the NdeI and XhoI sites to yield pLARS2. Then, L2CTD fused with the C-terminal FLAG tag (L2CTD-FLAG) was PCR-amplified from pLARS2. The linearized pLenti MTSGFP was fused with the DNA segment of L2CTD-FLAG using the SLiCE method to construct pLenti_L2CTD.

### Construction of MELAS myoblasts stably-overexpressing each factor

HEK293T cells were transfected with pLenti_MTO1_FLAG, pLenti_GTPBP3, or pLenti_L2CTD together with pMD2.G (Addgene #12259), pRSV-Rev (Addgene #12253), and pMDLg/pRRE (Addgene #12251) (67). Lentivirus for expressing each factor was prepared from the media used for culturing cells transduced with each pLenti vector constructed as described (68,69). Two μg of each pLenti vector containing the gene to be transduced, 7.5 μg of pMDLg/pRRE, 7.5 μg of pRSV-Rev, and 5 μg of pMD2.G, 2 ml of OPTi-MEM (Thermo Fisher) and 176 μl of PEI solution were mixed and left at room temperature for 20 min, and then HEK293T cells ($1.2 \times 10^7$) were transfected with the plasmid mixture, and cultured in 150 mm dish. The medium was replaced after 8–12 h, and 48 h after transfection, the medium was collected, then fresh medium was added, and 24 h later the medium was collected again. The recovered media were sterilized with a 0.22 μm PVDF filter (Millipore) and ultracentrifuged at 25 000 rpm for 1 h using SW28 to concentrate the virus. The recovered virus was suspended in PBS and stored at −80°C. The MELAS myoblasts with 3243A > G mutation were plated in 100 mm dishes and then transduced with each lentivirus. Twenty-four h after transduction, the medium was replaced with fresh medium, and the cells were cultured for 24 h, followed by addition of 2 μg/ml puromycin for selection. Within 3 weeks, puromycin-resistant cell colonies were picked and further expanded in the selection medium to obtain single cell-derived clones.

### Measuring the mutation rate of mtDNA by PCR-RFLP

Polymerase chain reaction-restriction fragment length polymorphism analysis (PCR-RFLP) (15,70) was performed to measure the 3242A > G mutation rate of mtDNAs in myoblasts. Cultured cells were lysed in lysis buffer [20 mM Tris–HCl (pH 8.0), 100 mM NaCl, 5 mM EDTA–NaOH (pH 8.0), and 0.1% SDS], followed by boiling at 60°C for 5 min and at 98°C for 2 min, and genomic DNA was extracted by phenol/chloroform/isoamyl alcohol (25:24:1) (Nacalai Tesque). The region including position 3243 of mtDNA was PCR-amplified with a set of primers (Supplementary Table S1). The PCR product was digested by the ApaI restriction enzyme and subjected to 10% native polyacrylamide gel electrophoresis (PAGE). Since 3243A > G mutation generates the ApaI site, the amplicon (666 bp) derived from mtDNA with the 3243A > G mutation was cleaved by ApaI into two fragments (234 and 432 bp). The gel was stained with SYBR Gold (S11494, Thermo Fisher Scientific), and the intensity of each band was quantified. The proportion of digested and undigested bands indicates the mutation rate of mtDNA with 3243A > G.

### Immunostaining

Cells were fixed with 3.7% formaldehyde, permeabilized with 1% Triton X-100, and blocked with 20% EzBlock Chemi (ATTO). Immunostaining was performed with the following primary antibodies: anti-FLAG (1:1000, mouse clone 1E6, 014-22383, Fujifilm) and anti-COXIV (1:100, rabbit polyclonal, 11242-1-AP, Proteintech). Antimouse IgG Alexa fluor 594 (1:1000, A11005, Invitrogen) or antirabbit IgG Alexa fluor 488 (1:1000, pA11008, Invitrogen) was used as a secondary antibody. To visualize DNA, the cells were stained with DAPI (1:1000). Images were acquired using a DMI 6000 B (Leica).

### RNA preparation

Each cell line cultured in a 100 mm dish was dissolved with 1 ml of homemade RNA isolation reagent [40% (w/v) phenol, 1% (v/v) ethylene glycol, 2 M guanidine thiocyanate, 0.1% (w/v) (6.9 mM) 8-quinolinol, 20 mM tri-sodium citrate dihydrate, 0.1 M NaOAc (pH 4.5), 0.1% (v/v) Triton X-100, 0.2% (w/v) *N*-lauroylsarcosine sodium salt, 50 mM salicylic acid, 10 mM Aluminon, and 0.0001% (w/v) Bromophenol Blue]. After vigorous shaking, chloroform was added to the solution at a concentration of 20%. The mixture was centrifuged, and the aqueous phase was collected, followed by two chloroform extractions for clarification. Total RNA was precipitated from the aqueous phase with 2-propanol.

### RT-qPCR

One μg of total RNA was incubated at 37°C for 30 min in a 10 μl solution containing 1× reaction buffer and 1 μl of RQ1 RNase-Free DNase (Promega). Then, 1 μl of 20 mM EGTA (pH8.0) was added, and the solution was boiled at 65°C for 10 min. The solution was mixed with 4 μl of 5× reaction buffer, 1 μl of 50 μM anchored-oligo$(dT)_{18}$ primer, and 2 μl of 600 μM random hexamers and then placed on ice for 5 min, followed by addition of 2 μl of 10× enzyme mix (EvoScript Reverse Transcriptase, Roche). RT was performed at 42°C for 15 min, followed by 85°C for 5 min and 65°C for 15 min, then diluted with 80 μl water. The cDNA solution (2.5 μl) was treated with 1 × KAPA SYBR Fast qPCR Master Mix (KAPA) and 0.2 μM of each primer. The PCR reaction was run on the Lightcycler 96 (Roche) with the following cycling conditions: 95°C for 180 s (1 cycle); 95°C for 10 s, 57°C for 20 s and 72°C for 1 s (40 cycles); 95°C for 5 s (1 cycle); 65°C for 60 s (1 cycle); 97°C for 1 s (1 cycle). Data were normalized to *GAPDH* mRNA. All primers used are listed in Supplementary Table S1.

### Western blotting

Myoblasts (2-4 × $10^6$) were lysed in 100 μl RIPA + EDTA buffer [50 mM Tris–HCl (pH 8.0), 150 mM NaCl, 1% NP-40, 0.5% sodium deoxycholate, 0.1% SDS, 1 mM EDTA, 1 mM DTT and 1× cOmplete, EDTA-free (Roche)]. The lysates were separated by 10% SDS-PAGE and electroblotted onto a PVDF membrane (Amersham Hybond P; GE Healthcare) using the Transblot Turbo apparatus (Bio-Rad). Western blotting was performed with the following primary antibodies: anti-MTO1 (1:1000, rabbit polyclonal, 15650-1-AP, Proteintech), anti-FLAG (1:2000, HRP-conjugated, PM020-7, MBL), anti-GTPBP3 (1:1000, rabbit polyclonal, HPA042158, Sigma-Aldrich), and anti-GAPDH (1:1000, mouse monoclonal, AM4300, Invitrogen). HRP-conjugated donkey antimouse IgG (1:20000, 715-035-150, Jackson ImmunoResearch) or HRP-conjugated donkey antirabbit IgG (1:20000, 711-035-152, Jackson ImmunoResearch) was used as a secondary antibody. Target proteins were detected using Pierce ECL Plus Western Blotting Substrate (Thermo Fisher Scientific) and visualized with ImageQuant LAS4000 mini (GE Healthcare). Bands were analyzed using ImageJ (National Institutes of Health).

### Isolation of mt-tRNA$^{Lys}$

Human mt-tRNA$^{Lys}$ was isolated from total RNA of myoblasts using the RCC method (71). DNA probes with a 5′-ethylcarbamate amino linker (Sigma-Aldrich) were covalently immobilized on NHS-activated Sepharose 4 Fast Flow (GE Healthcare) and packed into tip columns for the RCC instrument. The probe sequence is listed in Supplementary Table S1.

### Mass spectrometry

For RNA-MS, isolated mt-tRNA$^{Lys}$ was digested with RNase $T_1$ and analyzed by capillary LC and nanoESI MS as described in (72–74). A linear ion trap–orbitrap hybrid mass spectrometer (LTQ Orbitrap XL, Thermo Fisher Scientific) equipped with a custom-made nanospray ion source and a splitless nano-HPLC system (DiNA, KYA Technologies) was employed in this study. The percent frequency of each modification was calculated from the ratio of mass chromatogram peak areas of RNA fragments with and without the target modification.

For nucleoside analysis, bovine mt-tRNAs for Leu(UUR), Glu, and Gln isolated previously (35). Two to four micrograms of each isolated tRNA were reacted in a 20 μl mixture consisting of 5 μg/μl *N*-cyclohexyl-*N'*-β-(4-methylmorpholinium) ethylcarbodiimide (CMC) and 25 mM sodium carbonate buffer (pH 9.0) at room temperature under a light-shielded condition (75). Then, the nucleosides were analyzed using an LCQ ion trap (IT) mass spectrometer (ThermoFinnigan) equipped with an electrospray ionization (ESI) source and a MAGIC 2002 liquid chromatography system (Michrom BioResources). An ODS reversed-phase column with a 3 × 10 mm precolumn cartridge (Inertsil ODS-3, 2.1 × 250 mm; GL Sciences) was connected online to the electrospray interface. CID spectra were obtained using an LC/MS/MS experiment with a data-dependent scan.

### Measuring τm$^5$U frequency by CMC-PE

Detection of τm$^5$U sites by CMC-PE was performed as described for CMC-Ψ detection (73) with slight modifications. Fifteen μg of total RNA was dissolved in CMC solution [0.17 M *N*-cyclohexyl-*N'*-β-(4-methylmorpholinium) ethylcarbodiimide p-toluenesulfonate, 7 M urea, 50 mM Bicine, and 4 mM EDTA] and incubated at 37°C for 20 min. The

reaction was quenched by addition of 100 μl of stop solution [0.3 M NaOAc (pH 5.2), 0.1 mM EDTA (pH 8.0)] and recovered by two rounds of ethanol precipitation. The RNA pellet was rinsed with 70% EtOH and dried. The CMC-derivatized RNA was dissolved in 40 μl of 50 mM $Na_2CO_3$ (pH 10.4), incubated at 37°C for 4 h (alkaline treatment), ethanol precipitated, and dissolved in 10 μl of water. The DNA primers (Supplementary Table S1) were 5′-labeled with [γ-$^{32}$P] ATP (PerkinElmer, Inc) by T4 Polynucleotide Kinase (Toyobo) according to the manufacturer's instructions and centrifuged using a CENTRI-SEP spin column (Princeton Separations) to remove the labeled ATP. The treated RNA (0.75 μg) was mixed with the 5′-[$^{32}$P]-labeled primer (0.05 pmol) in a 5 μl solution containing 10 mM Tris–HCl (pH 7.7) and 1 mM EDTA (pH 8.0) and incubated at 80°C for 2 min, followed by incubation at room temperature. Subsequently, RT was started by adding 0.75 μl of water, 2 μl of 5 × FS buffer (Invitrogen), 0.25 μl of d/ddNTP mix containing 1.5 mM each of dATP and dTTP and 3.0 mM ddGTP, 1.5 μl of 25 mM $MgCl_2$, and 0.5 μl of SuperScriptIII (Invitrogen). The mixture was incubated at 55°C for 1 h. To stop the reaction and degrade the template RNA, 0.5 μl of 4 M NaOH was added to the reaction mixture, followed by boiling at 95°C for 5 min, and then the reaction was neutralized by addition of 14.5 μl of Loading Solution with Tris [12.5 μl of 2× loading solution for urea–PAGE, 1 μl of 1 M Tris and 1 μl of 1 M HCl] and incubation at 65°C for 5 min. The RT products were subjected to 20% PAGE with 7 M urea (20 × 20 cm$^2$, 0.35 mm). The gel was exposed to an imaging plate (BAS-MS2040, Fujifilm) to visualize the RT bands with the FLA-7000 fluorimager (Fujifilm). The band intensity was quantified by Multi Gauge (Fujifilm). The band intensity ratio of RT products was calculated by the sum of band intensities at positions 33 and 35 divided by the total sum of band intensities at positions 32, 33 and 35. To quantify the τm$^5$U frequency, CMC-PE was performed using total RNA mixtures of HeLa and *GTPBP3* KO cells at five different ratios (0:4, 1:3, 2:2, 3:1 and 4:0) to generate a calibration curve between the actual τm$^5$U frequency (0–96.3%) determined by RNA-MS (73) and the band intensity ratio of RT products (Figure 2C).

### Northern blotting

Total RNA (3 μg) from cultured cells was resolved by 10% PAGE containing 7 M urea, stained with ethidium bromide, blotted onto a nylon membrane (Amersham Hybond N+; GE Healthcare), dried, and cross-linked by UV (254 nm, 1200 J/cm$^2$). The DNA probe for mt-tRNA$^{Leu(UUR)}$ (Supplementary Table S1) was 5′-labeled with [γ-$^{32}$P] ATP (PerkinElmer) using T4 Polynucleotide Kinase (Toyobo). The membrane was subjected to hybridization at 50°C overnight in hybridization buffer [500 mM sodium phosphate buffer (pH 7.4), 7.5% SDS, 5% polyethylene glycol 6000, 1 mM EDTA–NaOH (pH 8.0), and 0.5% Casein] and 4 pmol of 5'-$^{32}$P-radiolabeled DNA probe. The membrane was washed three times with 1× SSC [150 mM NaCl, 15 mM Sodium citrate (pH 7.0)], dried, and exposed to an imaging plate (BAS-MS2040, Fujifilm) to visualize the hybridization bands using the FLA-7000 fluorimager (Fujifilm).

The *in vivo* aminoacylation status of mt-tRNA$^{Leu(UUR)}$ was analyzed by acid-urea northern blotting (76) with slight modifications. Total RNA was extracted under acidic conditions at low temperature as described previously (77). Three to ten μg of total RNA was resolved by 7.5% PAGE containing 7 M urea and 0.1 M NaOAc (pH 5.2) at 4°C overnight, blotted onto a nylon membrane, dried, and cross-linked by UV as described above. The DNA probes for mt-tRNA$^{Leu(UUR)}$ (Supplementary Table S1) were 5′-labeled with $^{32}$P, and northern blotting was performed as described above.

### Pulse-labeling of mitochondrial protein synthesis

Pulse-labeling of mitochondrial protein synthesis was performed as described previously (34). Myoblasts (4.0 × 10$^5$) were inoculated on 6-well plates and cultured at 37°C for 10 min with 1 ml of L-glutamine/L-cysteine-free DMEM (21013-024, Gibco) containing 10% dialyzed FBS (Gibco), 2 mM L-glutamine (Sigma) and 10 mM taurine, followed by addition of 50 μg/ml emetine to inhibit cytoplasmic protein synthesis and incubation for 10 min. Then, the cells were pulsed with 7.4 MBq (0.2 mCi) of [$^{35}$S] Met and [$^{35}$S] Cys (EXPRE$^{35}$S$^{35}$S Protein Labeling Mix, [$^{35}$S]-, PerkinElmer) and incubated at 37°C for 1 h to specifically label mitochondrial translation products. The medium was changed to DMEM-high glucose (D5796, Sigma-Aldrich) containing 10% dialyzed FBS (Gibco) and 10 mM taurine, and incubated for 10 min. Cell lysates (25 μg total proteins) were resolved by Tricine-SDS-PAGE (16.5%), and the gel was CBB-stained (CBB stain one, #04543-51, Nacalai Tesque) and dried on a gel drier (AE-3750 RapiDry, ATTO). The dried gel was exposed to an imaging plate (BAS-MS2040, Fujifilm) to visualize the radiolabeled bands using the FLA-7000 fluorimager (Fujifilm).

### Oxygen consumption rate

An XFe24 extracellular flux analyzer (Seahorse Bioscience) was used to measure the oxygen consumption rate (OCR) and extracellular acidification rate (ECAR). Myoblasts (1 × 10$^5$) were seeded in four wells of the XFe24 cell culture miniplate precoated with collagen (Seahorse Bioscience) and cultured at 37°C for 24 h. The medium was then replaced with DMEM (D5523, Sigma) containing 25 mM glucose, 1 mM sodium pyruvate, and 4 mM L-glutamine (adjusted to pH 7.4 with NaOH). The OCR of each well was measured over the course of programmed injections of oligomycin (f.c. 1.0 μM), carbonyl cyanide-p-trifluoromethoxyphenylhydrazone (FCCP) (f.c. 2.0 μM), and rotenone/antimycin A (f.c. 0.5 μM). Basal respiration was determined as the OCR before oligomycin minus the minimum OCR after rotenone/antimycin A (nonmitochondrial OCR). Maximal respiration was determined as the maximum OCR after FCCP minus the nonmitochondrial OCR. ATP-linked respiration was determined as the OCR before oligomycin minus the minimum OCR after oligomycin. Spare respiration capacity was determined as the difference between maximal OCR after FCCP and basal OCR.

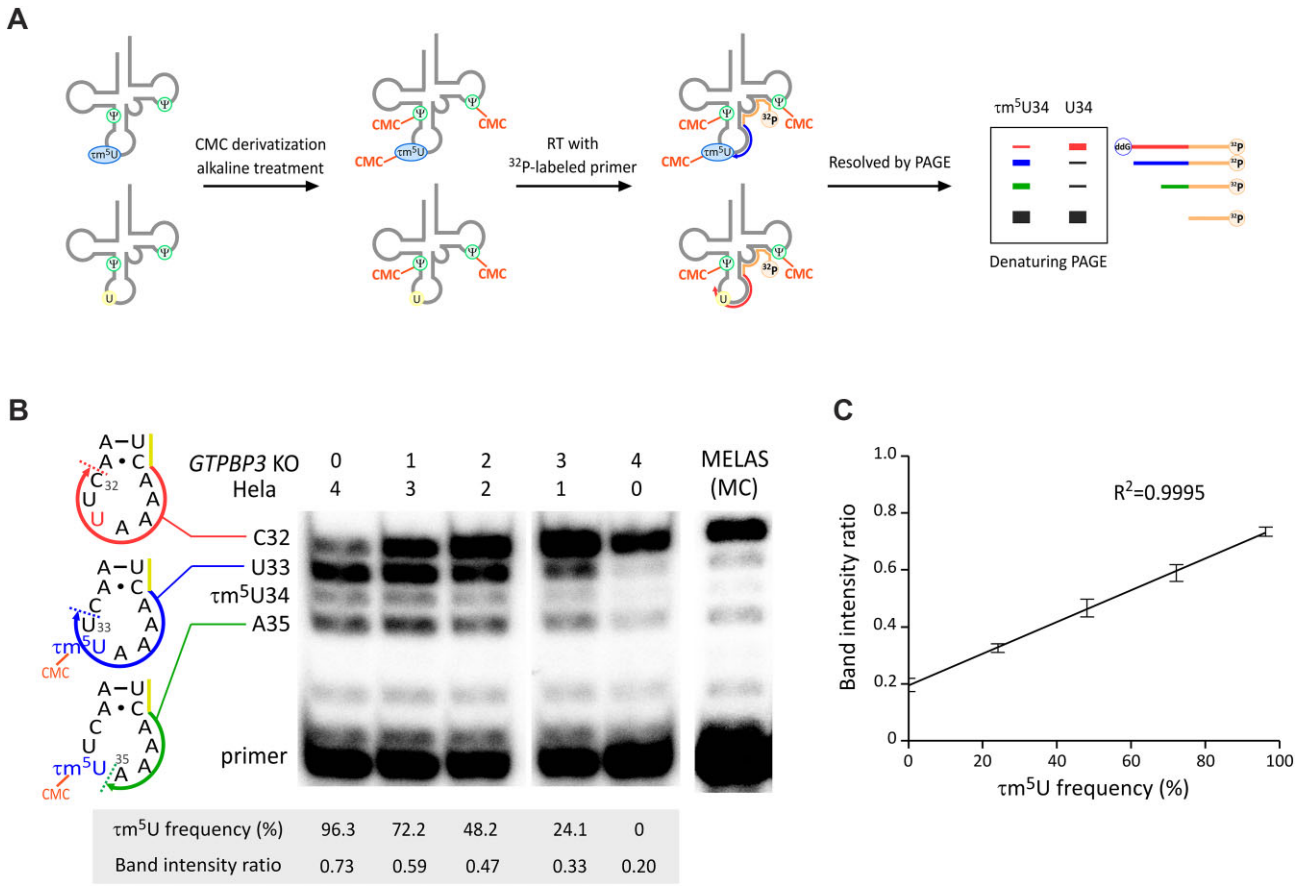


**Figure 2.** Measuring $\tau m^5U$ frequency in mt-tRNA$^{Leu(UUR)}$ by CMC-PE. (**A**) Schematic of CMC-PE. The detailed procedure is described in the 'MATERIALS AND METHODS' section. (**B**) cDNA bands of CMC-PE for $\tau m^5U34$ of mt-tRNA$^{Leu(UUR)}$ in total RNA mixtures of HeLa and *GTPBP3* KO cells at different mixing ratios. CMC-PE for the MELAS patient myoblasts bearing 3243A > G (MC cell line) was also performed. When mt-tRNA$^{Leu(UUR)}$ has no $\tau m^5U34$, the cDNA stops at position 32 through the insertion of dideoxyguanosine (red arrow). When mt-tRNA$^{Leu(UUR)}$ is fully modified with $\tau m^5U34$, the cDNA is stopped at positions 33 (blue arrow) and 35 (green arrow) by CMC-$\tau m^5U34$. A part of primer is indicated by the yellow line. $\tau m^5U$ frequency and band intensity ratio for each lane are shown below the gel image. (**C**) Calibration line of CMC-PE for $\tau m^5U34$ of mt-tRNA$^{Leu(UUR)}$ in total RNA mixtures of HeLa and GTPBP3 KO cells at different mixing ratios. The band intensity ratios were calculated as described in 'MATERIALS AND METHODS.' Data represent the average values of technical triplicates ± s.d. ($R^2 = 0.9995$).

## RESULTS

### Highly sensitive detection and quantification of the $\tau m^5U$ modification by CMC-PE

We previously optimized a primer extension (PE) method and successfully measured $\tau m^5U$ frequency in mt-tRNAs$^{Leu(UUR)}$ with several pathogenic mutations from clinical specimens of MELAS patients (33). In this PE method, $\tau m^5U34$ does not simply inhibit reverse transcription (RT) but somehow interferes with cDNA extension after a reverse transcriptase (RTase) passes by the modification site, resulting in a cDNA band arrested at position 33. Here, we report a novel PE method named CMC-PE to detect more robustly and quantify $\tau m^5U34$ in mt-tRNA$^{Leu(UUR)}$.

Pseudouridine (Ψ) and some modified uridines are derivatized by *N*-cyclohexyl-*N*′-β-(4-methylmorpholinium)ethylcarbodiimide (CMC) to form a stable CMC-adduct under basic conditions (75,78,79). The sites of CMC-Ψ can be detected by PE (80) or deep sequencing (81), indicating that $\tau m^5U$ can be detected by CMC derivatization. We first analyzed the chemical structure of CMC-$\tau m^5U$ by collision-induced dissociation (CID) (Supplementary Figure S1A). Assignment of the product ions indicated that CMC is attached to a nitrogen atom of the taurine moiety in $\tau m^5U$ (Supplementary Figure S1A). We also analyzed CMC-$\tau m^5s^2U$ by CID and found that CMC is attached to the nitrogen atom at the same position as CMC-$\tau m^5U$ (Supplementary Figure S1B). To detect CMC-$\tau m^5U$ by PE, total RNAs from HeLa and *GTPBP3* KO cells were reacted with CMC, followed by mild alkaline treatment to hydrolyze CMC-adducts of uridines and guanosines. Then, a 5′-[$^{32}$P]-labeled DNA primer was hybridized to mt-tRNA$^{Leu(UUR)}$ in total RNA, and PE was performed to detect the RT stop induced by CMC-$\tau m^5U$ (Figure 2A). When mt-tRNA$^{Leu(UUR)}$ from HeLa cells was analyzed by PE, we observed three major cDNA bands corresponding to positions 32, 33 and 35 (Figure 2B), whereas two lower bands corresponding to positions 33 and 35 were missing in mt-tRNA$^{Leu(UUR)}$ from *GTPBP3* KO cells (Figure 2B). Because $\tau m^5U$ does not occur in *GTPBP3* KO cells (34), the cDNA extends through

the anticodon region and stops at position 32 by inserting dideoxy guanosine, resulting in one strong band at this position (Figure 2B). These results suggest that CMC-$\tau m^5U$ acts as a roadblock to produce two lower bands corresponding to positions 33 and 35 (Figure 2B). The band at position 33 is also produced by the original PE method (33), whereas the band at position 35 is only produced by CMC treatment, indicating that the bulky side chain of CMC-$\tau m^5U$ hinders cDNA extension. Mass spectrometric analysis of mt-tRNA$^{Leu(UUR)}$ isolated from HeLa cells (34) estimates the $\tau m^5U34$ modification frequency to be 96.3%. To quantify the $\tau m^5U$ frequency of MELAS tRNA by CMC-PE, we mixed total RNAs from HeLa and *GTPBP3* KO cells at five different ratios (0:4, 1:3, 2:2, 3:1 and 4:0) and performed CMC-PE to generate a calibration curve between $\tau m^5U$ frequency (0–96.3%) and the band intensity ratio of RT products, which was calculated by the sum of band intensities at positions 33 and 35 divided by the total sum of band intensities at positions 32, 33, and 35 (Figure 2C). This resulted in clean linearity ($R^2 = 0.9995$), which enabled the quantification of $\tau m^5U$ frequency in MELAS tRNA. We next performed CMC-PE for mutant mt-tRNA$^{Leu(UUR)}$ derived from MELAS patient myoblasts (MC cell line) bearing 3243A > G with a 98.4% mutation rate (Figure 2B), and the $\tau m^5U$ frequency was measured as 16.3% using the calibration line. These results confirmed a severe reduction of $\tau m^5U$ frequency in MELAS tRNA.

### Overexpression of *MTO1* or *GTPBP3* in MELAS myoblasts with the 3243A > G mutation

Our findings that MELAS tRNAs have a low frequency of $\tau m^5U$ modification (33) suggest that each MELAS mutation prevents tRNA recognition by $\tau m^5U$-modifying enzymes (82). We hypothesized that overexpression of *MTO1* or *GTPBP3* might introduce a $\tau m^5U$ modification to activate MELAS tRNA, thereby restoring mitochondrial function in MELAS patient cells. To test this, we constructed stable cell lines of MELAS myoblasts overexpressing *MTO1* or *GTPBP3*. The MELAS myoblasts were transduced with a lentiviral vector harboring a gene encoding C-terminally FLAG-tagged *MTO1* or *GTPBP3* under the CMV promoter. We isolated a single clone that stably overexpressed *MTO1* or *GTPBP3*, and obtained two cell lines (MM1#1 and MM1#2) for *MTO1* overexpression and one cell line (MG3) for *GTPBP3* overexpression. In addition, we generated a cell line overexpressing the C-terminal domain of *LARS2* (L2CTD, 78 amino acids) (ML2) and a control cell line of MELAS myoblasts stably expressing *GFP* (MC). The mutation rate of mtDNA was measured by PCR-RFLP (Supplementary Figure S2A), and the results showed that the high rate of 3243A > G mutation (95.6–98.8%) was maintained in each cell line.

Overexpression of *MTO1* was confirmed in both MM1#1 and MM1#2 cells by western blotting (Figure 3A) and RT-qPCR (Supplementary Figure S2B). Mitochondrial localization of MTO1 was also confirmed (Figure 3B). In the MG3 cells, *GTPBP3* overexpression was detected by western blotting (Figure 3A) and RT-qPCR (Supplementary Figure S2B). The N-terminal mitochondrial targeting sequence (MTS) of GTPBP3 was partially cleaved in mitochondria (Figure 3A). In the ML2 cells, the expression and mitochondrial localization of L2CTD were confirmed using an anti-FLAG antibody (Figure 3B).

### Characterization of MELAS tRNA in myoblasts overexpressing *MTO1*

CMC-PE for MELAS tRNA with the 3243A > G mutation was performed in each cell line. For efficient uptake of taurine into the cells, the cells were cultured in the medium supplemented with 10 mM taurine. According to the band intensity ratio of RT products, the $\tau m^5U$ frequency was measured for each cell line using the calibration line (Figure 2C). The $\tau m^5U$ frequency of MELAS tRNA in *GTPBP3* KO, HeLa, and MC cells were 0%, 96.3% and 16.3%, respectively (Figure 3C). WT myoblasts with a low rate of 3243A > G mutation (0.76%) were cultured as the MELAS myoblast parental cell line (Supplementary Figure S2A). The mt-tRNA$^{Leu(UUR)}$ from WT myoblasts was fully modified with $\tau m^5U$ (∼100%) (Figure 3C). Overexpression of *MTO1* drastically increased the $\tau m^5U$ frequency of MELAS tRNA to 97.3% in MM1#1 and 94.8% in MM1#2 (Figure 3C). To examine whether the taurine supplementation in the culture medium affected the recovery of $\tau m^5U$ of MELAS tRNA together with *MTO1* overexpression, we analyzed the $\tau m^5U$ frequency of WT, MC, MM1#1 and MM1#2 cells cultured in the medium without taurine supplementation (Supplementary Figure S3). When compared to 10 mM taurine supplementation, we observed a slight decrease in the $\tau m^5U$ frequency in WT cells cultured without taurine supplementation, whereas the $\tau m^5U$ frequency of the MELAS tRNA was almost completely restored by *MTO1* overexpression irrelevant with or without taurine supplementation (Supplementary Figure S3).

The $\tau m^5U$ frequency of MELAS tRNA increased slightly to 27.3% in the MG3 cells and to 27.7% in the ML2 cells (Figure 3C). Overexpression of these factors had a marginal effect on $\tau m^5U$ introduction to MELAS tRNA. These results demonstrated that *MTO1* overexpression effectively restored the $\tau m^5U$ modification in MELAS tRNA.

Next, we performed northern blotting to measure the steady-state levels of mt-tRNA$^{Leu(UUR)}$ in each cell line. Consistent with a previous report (21), the steady-state level of MELAS tRNA in the MC cells decreased to 37.4% of that in WT tRNA (Figure 4A and B). There was no significant difference in the steady-state level of MELAS tRNA between cell lines (Figure 4A and B). Neither *MTO1* nor *GTPBP3* overexpression stabilized the MELAS tRNA. Even when the C-terminal domain of *LARS2* was overexpressed, there was little change in the steady-state level of MELAS tRNA. These observations suggest that overexpression of these factors failed to stabilize MELAS tRNA.

MELAS mutation reduces the aminoacylation efficiency (21,26,27). We thus examined the effect of *MTO1* overexpression on aminoacylation of MELAS tRNA. To this end, we analyzed the *in vivo* aminoacylation status of mt-tRNA$^{Leu(UUR)}$ in each cell line by acid-urea northern blotting (76). The *in vivo* aminoacylation level of MELAS tRNA in the MC cells was reduced to 30.4% of that in WT tRNA (Figure 4C). Overexpression of *MTO1* slightly but significantly increased the aminoacylation level of MELAS

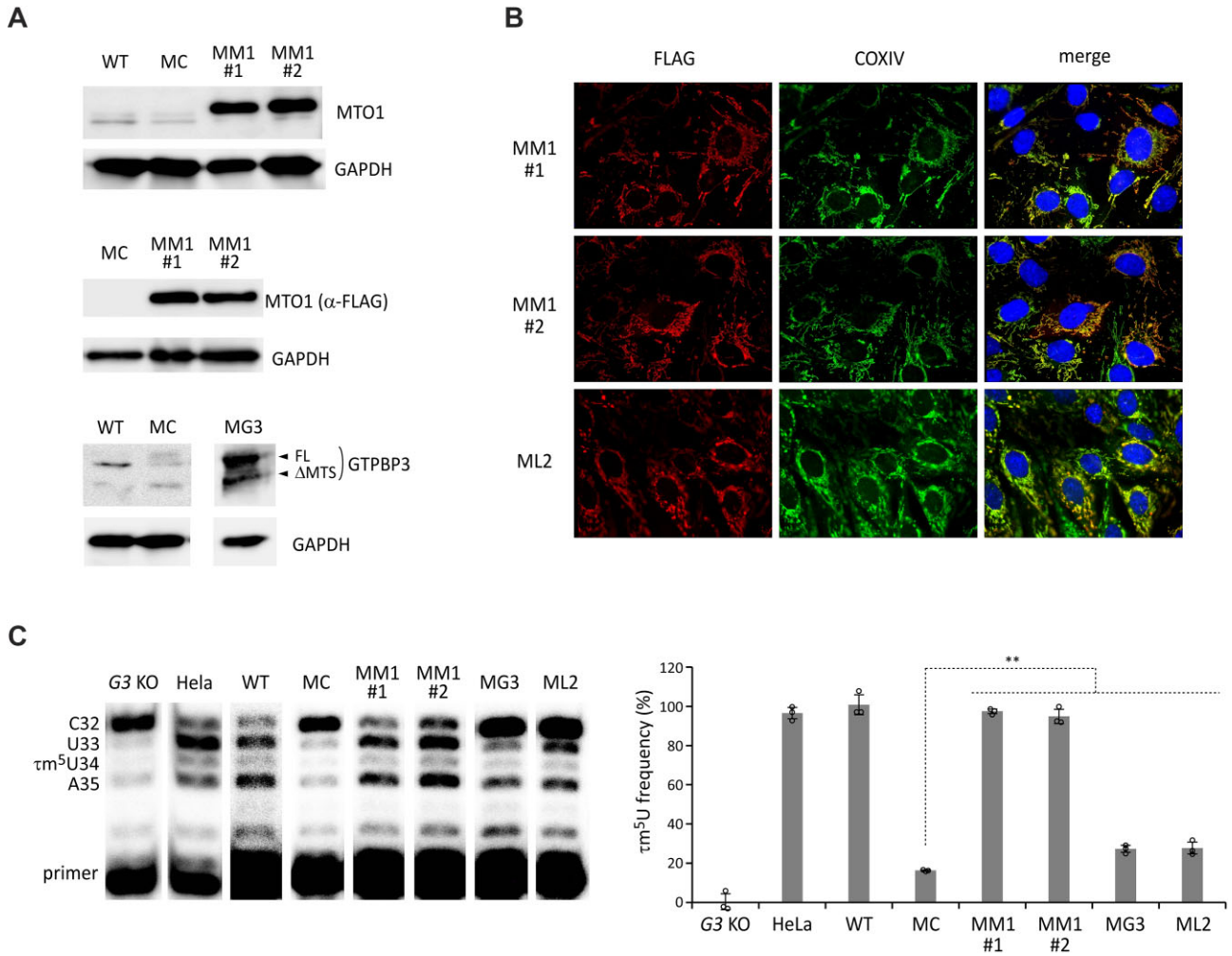


**Figure 3.** Restoration of $\tau m^5U$ in mt-tRNA$^{Leu(UUR)}$ by *MTO1* overexpression in MELAS myoblasts. (**A**) Western blotting of MTO1 with an anti-MTO1 antibody (upper), MTO1-FLAG with an anti-FLAG antibody (middle), and GTPBP3 with an anti-GTPBP3 antibody (lower) in the indicated myoblasts: WT (parental line), MC (MELAS control cells), MM1#1 and MM1#2 (*MTO1* overexpression cells), MG3 (*GTPBP3* overexpression cells) and ML2 (*L2CTP* overexpression cells). GAPDH was used as the loading control. (**B**) Immunostaining of MM1 cells by MTO1-FLAG (upper and middle panels) and the ML2 cells by L2CTD-FLAG (bottom panels) with anti-FLAG antibody (red) and anti-COXIV antibody (green). Nuclei were stained with DAPI (blue). All images were superimposed to generate the merged panels (right panels). (**C**) Measuring the $\tau m^5U$ frequency of mt-tRNA$^{Leu(UUR)}$ by CMC-PE in various cell lines. CMC-PE was performed in the indicated cell lines (left panel). The $\tau m^5U$ frequency in each cell line was calculated by the band intensity ratio using the standard line (Figure 2C) (right panel). *G3* KO stands for *GTPBP3* KO cell line. Data represent the average values of technical triplicates ± s.d. $^{**}P < 0.01$, Student's *t*-test.

tRNA in both cell lines (41.8% in MM1#1 and 50.5% in MM1#2) (Figure 4C), suggesting that *MTO1* overexpression partially rescues the aminoacylation status of MELAS tRNA with the 3243A > G mutation.

### *MTO1* overexpression restores mitochondrial activity in MELAS myoblasts

To evaluate mitochondrial protein synthesis, we performed a pulse-labeling experiment. Cytoplasmic protein synthesis was inhibited by emetine, and nascent proteins synthesized in mitochondria were labeled with [$^{35}$S] Met and Cys for 1 h, resolved by Tricine-SDS-PAGE, and the labeled proteins were visualized (Figure 4D) and quantified (Figure 4E). Most proteins encoded in mtDNA were detected (Figure 4D). The band intensities of mitochondrial proteins were markedly lower in the MC cells than in the WT cells (Figure 4D and E). The band intensity of each protein was combined to compare total mitochondrial protein synthesis (Figure 4E), which showed a 48.9% reduction in the mitochondrial translation efficiency of the MC cells compared with that of the WT cells. Overexpression of *MTO1* increased the band intensity of each protein; in particular, Cytb, ATP6, ND3 and ND4L or ATP6 were fully restored to the WT level (Figure 4E). Total mitochondrial protein synthesis in MM1 cells recovered to 79–92% of that in the WT cells (Figure 4E).

We next examined the effect of *MTO1* overexpression on the respiratory activity of MELAS myoblasts. To examine the mitochondrial function of each cell line, we monitored the oxygen consumption rate (OCR) and extracellular acidification rate (ECAR) using a flux analyzer (Figure 5A and B). OCR and ECAR were recorded under basal conditions, followed by addition of a series of inhibitors of respiratory

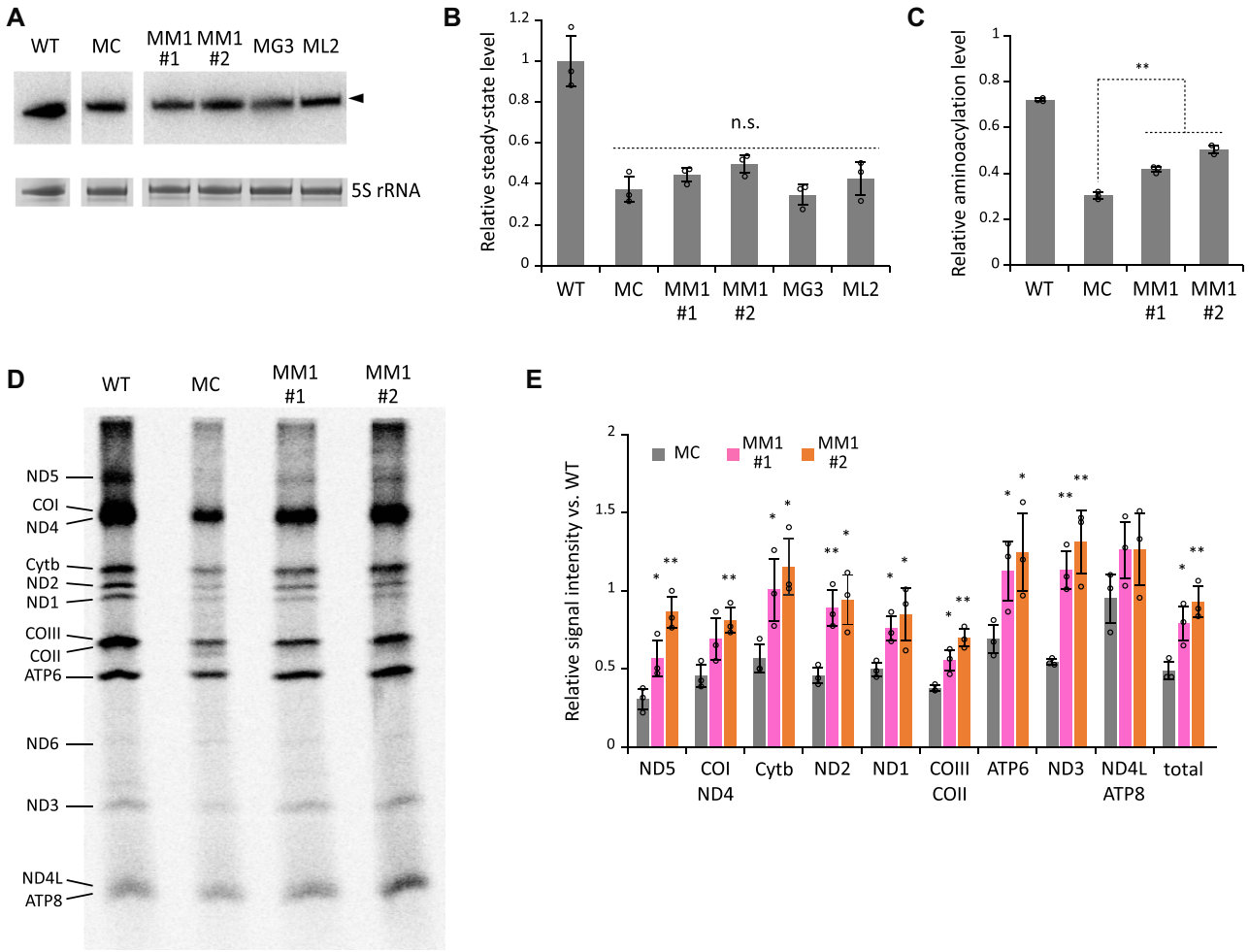


**Figure 4.** Effect of *MTO1* overexpression on mt-tRNA$^{Leu(UUR)}$ and mitochondrial translation in MELAS myoblasts. (**A**) Steady-state level of mt-tRNA$^{Leu(UUR)}$ in a series of myoblasts measured by northern blotting. The bands corresponding to mt-tRNA$^{Leu(UUR)}$ are marked by an arrow (upper panel). 5S rRNAs stained with EtBr are used as loading controls (lower panel). (**B**) Relative steady-state level of mt-tRNA$^{Leu(UUR)}$ in each cell line normalized to that in the WT. Data represent the average values of technical triplicates ± s.d. (**C**) Aminoacylation levels of mt-tRNA$^{Leu(UUR)}$ in a series of myoblasts measured by acid-urea northern blotting. Data represent the average values of three independent samples ± s.d. $^{**}P < 0.01$, Student's *t*-test. (**D**) Pulse-labeling experiment of mitochondrial protein synthesis. WT, MC, MM1#1 and MM1#2 cells were pulse-labeled with [$^{35}$S]-labeled Met and Cys after cytoplasmic translation was halted by emetine. The assignment of mitochondrial proteins is indicated on the left. (**E**) The band intensity ratios of each mitochondrial protein in MC (gray), MM1#1 (pink), and MM1#2 (orange) relative to those in the WT. The relative intensity of total mitochondrial proteins is shown on the right. CBB-stained gel images are shown in Source Data. Data represent the average values of three independent samples ± s.d. $^{*}P < 0.05$; $^{**}P < 0.01$, Student's *t*-test versus MC.

chain complexes at the indicated time points (Figure 5A and B). The basal respiration, ATP production, maximal respiration, and spare respiration capacity values of each cell line were calculated based on OCR changes during the measurement (Figure 5C). The MC cells showed a lower OCR than the WT even under basal conditions (Figure 5A). ECAR in the MC cells did not increase after inhibition of ATP synthesis (Figure 5B), suggesting that mitochondrial activity was severely impaired in MELAS myoblasts. Overexpression of *MTO1* significantly increased all mitochondrial activity values in both MM1 cell lines (Figure 5C), although those values did not reach WT levels (Figure 5C). Inhibition of mitochondrial ATP synthesis by oligomycin increased ECAR in both MM1 cell lines (Figure 5B), indicating that cellular ATP production shifts to anaerobic glycolysis, producing more lactate and thereby acidifying the medium. These observations strongly suggest that ATP synthesis in MM1 cells depends not only on anaerobic glycolysis but also on mitochondrial activity.

Taken together, these findings indicate that *MTO1* overexpression increases $\tau m^5U$ frequency to activate MELAS tRNA, thereby restoring mitochondrial protein synthesis and respiratory activity.

### Restoring the taurine modification of MERRF tRNA by *MTO1* overexpression

We previously reported hypomodification of $\tau m^5s^2U$ in mt-tRNA$^{Lys}$ with the 8344A > G mutation in MERRF patient cells (Figure 1B) (44,45), which suggests that the MERRF mutation impairs tRNA recognition by the MTO1 and GTPBP3 complex responsible for 5-taurinomethyl modi-

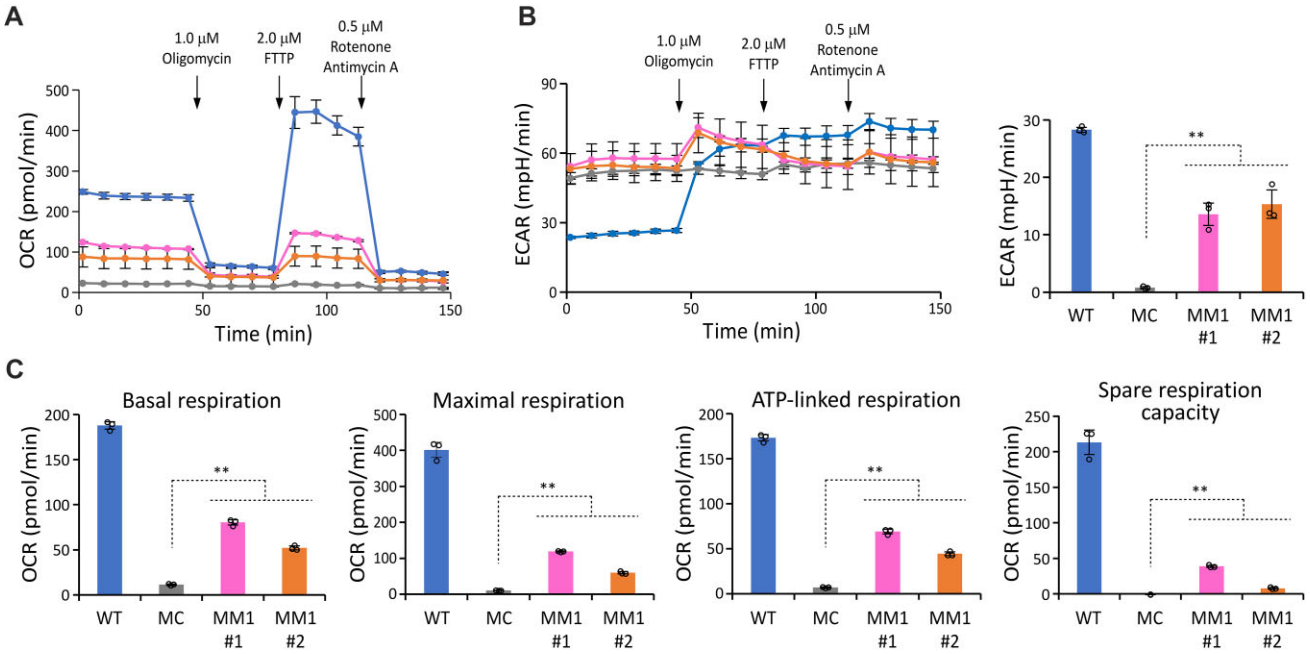


**Figure 5.** Effect of *MTO1* overexpression on respiration in MELAS myoblasts. (A, B) Oxygen consumption rate (OCR) (**A**) and extracellular acidification rate (ECAR) (**B**) in WT (blue), MC (gray), MM1#1 (pink), and MM1#2 (orange) measured with the Seahorse XFe24 extracellular flux analyzer. Inhibitors were sequentially added at the indicated times. The right graph in (B) shows the difference in ECAR between before and after the addition of oligomycin. Data represent the average values of three independent samples ± s.d. (**C**) Basal respiration, maximal respiration, ATP production, and spare respiration capacity in the four myoblasts. Data represent the average values of three independent samples ± s.d. $*P < 0.05$; $**P < 0.01$, Student's *t*-test.

fication as well as by MTU1 responsible for 2-thiouridine modification (5,82). $m^1A58$ is a partial modification of human mt-$tRNA^{Lys}$ (Figure 1B) that is introduced by TRMT61B (63). It was reported that $m^1A58$ is also missing in MERRF tRNA (47). Overexpression of *TRMT61B* increases $m^1A58$ in the MERRF tRNA and restores mitochondrial protein synthesis in MERRF myoblasts (47). *MTO1* overexpression also restores mitochondrial protein synthesis in MERRF myoblasts (47), although the $\tau m^5s^2U$ status has not been analyzed.

To analyze the tRNA modification status of MERRF tRNA more precisely, we employed RNA mass spectrometry (RNA-MS) (73) to measure the frequency of tRNA modifications of mt-$tRNA^{Lys}$ isolated from cell lines used in previous studies (47). We isolated mt-$tRNA^{Lys}$ from WT and MERRF 8344A > G myoblasts by reciprocal circulating chromatography (RCC) (71) and analyzed the anticodon-containing fragments with different modification status (Figure 6A). The frequencies of $\tau m^5s^2U34$ and $\tau m^5U34$ in WT mt-$tRNA^{Lys}$ were 8.9% and 6.0%, respectively (Figure 6A). In MERRF mt-$tRNA^{Lys}$ with the 8344A > G mutation, both $\tau m^5s^2U34$ and $\tau m^5U34$ were severely reduced to 0.2%, instead $s^2U34$ and U34 increased to 28.7% and 71.0%, respectively (Figure 6A). Overexpression of *MTO1* in MERRF myoblasts drastically increased the frequencies of $\tau m^5s^2U34$ and $\tau m^5U34$ to 14.2% and 27.7%, respectively, whereas $s^2U34$ and U34 decreased to 12.8% and 45.2%, respectively (Figure 6A).

Next, we analyzed $m^1A58$ in mt-$tRNA^{Lys}$ from WT and MERRF 8344A > G myoblasts. The frequency of $m^1A58$ was 25.7% in WT tRNA (Figure 6B) and 1.0% in MERRF tRNA (Figure 6C). Overexpression of *TRMT61B* increased the frequency of $m^1A58$ to 85.3% in WT tRNA (Figure 6B) and 87.2% in MERRF tRNA (Figure 6C), consistent with those obtained by the primer extension-based method in the previous study (47). *TRMT61B* overexpression resulted in a small change in anticodon modifications (Figure 6A). Likewise, *MTO1* overexpression did not affect the $m^1A58$ modification in MERRF tRNA (Figure 6C). These observations suggest that *MTO1*-mediated taurine modification and *TRMT61B*-mediated $m^1A58$ modification do not affect each tRNA modification. Thus, overexpression of *MTO1* or *TRMT61B* introduces the respective tRNA modifications to activate MERRF tRNA independently, thereby restoring mitochondrial translation and respiratory activity.

## DISCUSSION

RNA modifications are not static but rather change dynamically in response to various cellular processes including development, differentiation, metabolic alterations, environmental stresses, and diseases (82–85). The biological roles of tRNA modifications have recently attracted attention in many research areas. tRNAs contain a wide variety of modifications in the anticodon regions. These modifications are important for accurate and efficient protein synthesis, thereby contributing to codon optimality related to proteostasis and mRNA stability (86–88). Deficiency in tRNA modifications causes various diseases, highlighting the physiological importance of these modifications (5,82,89,90).

Understanding the tRNA modification status under specific conditions requires a highly sensitive analytical method to accurately and comprehensively assess and profile tRNA

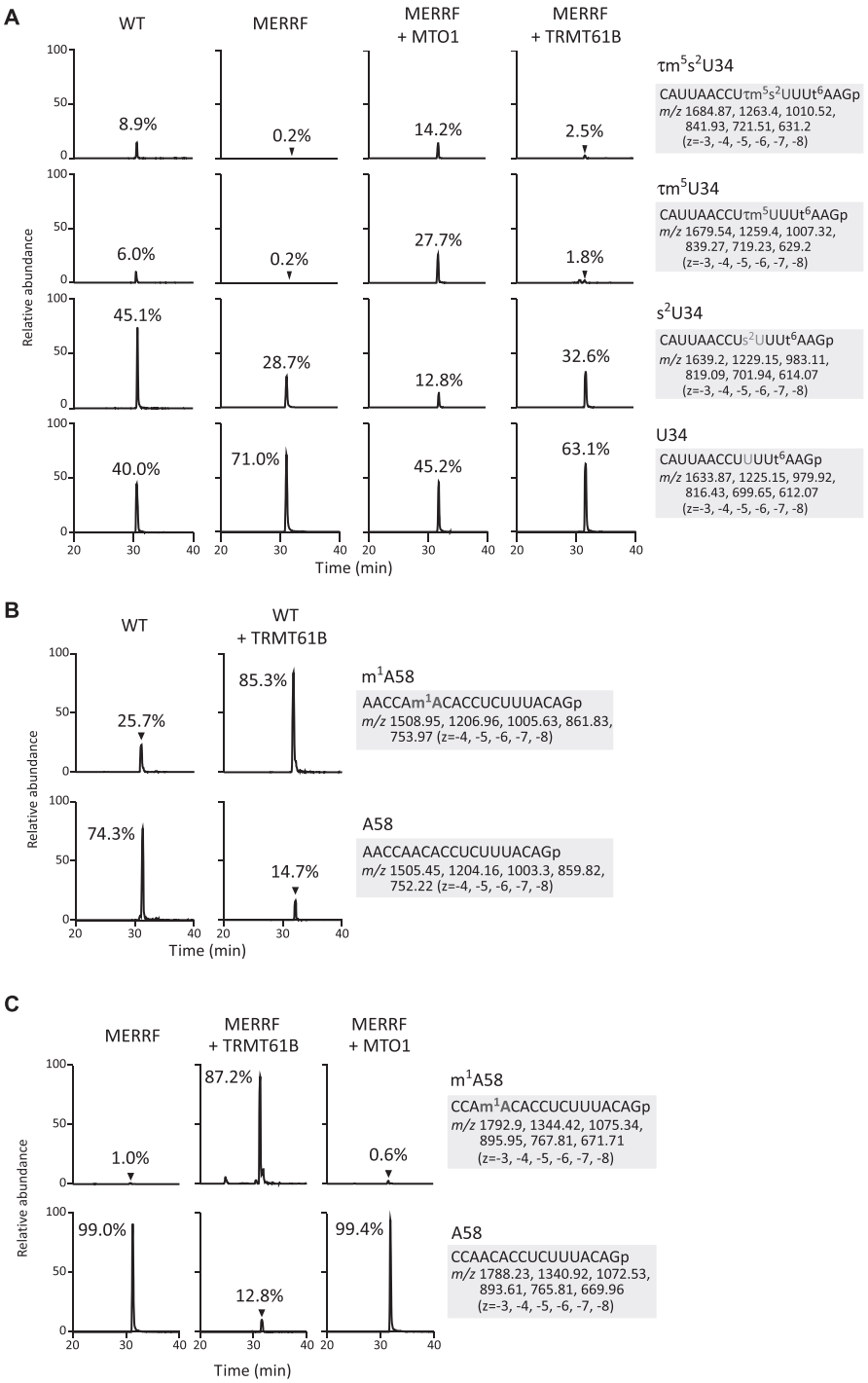


**Figure 6.** Restoration of tRNA modifications of mt-tRNA$^{Lys}$ with the 8344A > G mutation by overexpression of *MTO1* or *TRMT61B* in MERRF myoblasts. (**A**) Extracted ion chromatograms (XICs) of the RNase $T_1$-digested fragments of mt-tRNA$^{Lys}$ with different anticodon modification status for WT myoblasts (left panels), MERRF myoblasts with empty vector (second panels), MERRF myoblasts with *MTO1* overexpression (third panels), and MERRF myoblasts with *TRMT61B* overexpression (right panels). The sequences of the detected fragments with $m/z$ values and charge states are indicated on the right. The relative $\tau m^5(s^2)U$ frequencies indicated in chromatograms were calculated from the peak area ratio of the multiply charged negative ions (−3 to −8) for RNA fragments with different modifications. (**B**) XICs of $m^1A58$-containing fragments with (upper panels) or without (lower panels) the $m^1A$ modification of mt-tRNA$^{Lys}$ isolated from WT myoblasts transfected with empty vector (left panels) or *TRMT61B* (right panels). The sequences of the detected fragments, the $m/z$ values and charge states are indicated on the right. The relative $m^1A$ frequencies indicated in chromatograms were calculated from the peak area ratio of the multiply charged negative ions (−4 to −8) for RNA fragments with or without the modification. (**C**) XICs of $m^1A58$-containing fragments with (upper panels) or without (lower panels) $m^1A$ modification of mt-tRNA$^{Lys}$ isolated from MERRF myoblasts transfected with empty vector (left panels), *TRMT61B* (middle panels), or *MTO1* (right panels). The sequence of the detected fragments with $m/z$ values and charge states are indicated on the right. The relative $m^1A$ frequencies indicated in chromatograms were calculated from the peak area ratio of the multiply charged negative ions (−3 to −8) for RNA fragments with or without the modification.

modifications using limited amounts of tissues or clinical specimens. RNA-MS is a highly sensitive and powerful analytical method capable of detecting and quantifying RNA modifications accurately and reliably (72,73,91,92). In particular, RNA-MS is suitable for analyzing total nucleosides to quantify global alterations of RNA modifications in multiple analytes (72,91,93–95). However, to analyze the RNA modification status at given sites of individual RNAs, it is necessary to isolate and purify the target RNA molecule for RNA-MS (71,73). In general, RNA isolation is not a simple method and requires large amounts of specimens, complex procedures, and technical skill and expertise. Sequencing-based methods are highly sensitive and suitable for detecting several RNA modifications in a transcriptome-wide manner using a limited quantity of specimens, although this method is applicable only to specific RNA modifications (96–98). Several RNA modifications can be detected by cDNA arrest or misincorporation during cDNA synthesis by reverse transcriptase (RTase) (96,99). For some RNA modifications that do not interfere with the RT reaction, various approaches such as chemical derivatizations, partial cleavage by nuclease, and reduced NTP concentration have been developed to detect certain RNA modifications in a transcriptome-wide manner (96,99). However, there remain a number of RNA modifications that cannot be detected by RTase-based techniques.

Various types of uridine modifications are present at the first position of the anticodon of tRNAs, and play critical roles in accurate and efficient decoding during protein synthesis (82,100). However, there are no general and practical RTase-based methods to detect these uridine modifications because they do not interfere with the RT reaction in general. We previously developed a PE-based method to detect the $\tau m^5U$ modification using MMLV RTase (33). This method requires careful optimization of PE conditions, and no other RTases are available for this method. We previously showed that CMC forms a stable adduct with some uridine modifications in addition to Ψ (75); here, we succeeded in robustly and quantitatively detecting $\tau m^5U$ of mt-tRNA$^{Leu(UUR)}$ using CMC-PE (Figure 2). In principle, CMC-PE has the potential to detect other uridine modifications, thus expanding the application range of CMC-PE. Although we used a radio isotope (RI)-labeled primer for CMC-PE, further studies will enable the establishment of a non-RI system of CMC-PE by quantifying the cDNA products by qPCR or deep sequencing for the highly sensitive analysis of limited amounts of specimens. We expect that CMC-PE will be applied to clinical specimens to quantify $\tau m^5U$ frequency for the diagnosis of mitochondrial diseases.

In this study, we successfully increased the frequency of $\tau m^5U$ in MELAS tRNA from 16% to 95–97% by overexpressing *MTO1* in MELAS myoblasts (Figure 3C). There was no significant difference in the restoration of $\tau m^5U$ modification by *MTO1* overexpression with or without taurine supplementation to the culture medium (Supplementary Figure S3). This result also indicated that the amount of taurine in the medium, which is estimated to be about 2 μM in 10% FBS (101), was sufficient for $\tau m^5U$ formation on mt-tRNA$^{Leu(UUR)}$. The MELAS mutations, represented by 3243A > G, destabilize the tRNA tertiary structure, decreasing steady-state levels, aminoacylation status, and tRNA modification frequency (21,33). Although human mt-tRNA$^{Leu(UUR)}$ has nine modification sites (Figure 1A), only $\tau m^5U$ is commonly impaired in MELAS tRNAs (33), suggesting that MELAS mutations not only destabilize the tRNA structure but also prevent tRNA recognition by $\tau m^5U$-modifying enzymes (MTO1 and GTPBP3 complex). Bacterial tRNAs and yeast or nematode mt-tRNAs have 5-carboxymethylaminomethyluridine ($cmnm^5U$) instead of $\tau m^5U$ (102,103). $cmnm^5U$ is a uridine modification in which the taurine moiety of $\tau m^5U$ is replaced by glycine. MnmG and MnmE, which are homologous enzymes of MTO1 and GTPBP3, synthesize the $cmnm^5U$ modification in the presence of glycine and $CH_2$-THF as substrates, using GTP, FAD, NADH and $K^+$ as cofactors (34,104,105). Although the detailed reaction mechanism catalyzed by these enzymes remains elusive, MnmG shares amino acid sequence similarity with the folate-dependent tRNA methyltransferase TrmFO, which directly recognizes tRNA (106,107). Given that MELAS mutations likely impair tRNA recognition by $\tau m^5U$-modifying enzymes, it is reasonable that *MTO1* overexpression drastically increased the $\tau m^5U$ frequency of mt-tRNA$^{Leu(UUR)}$ by overcoming the MELAS mutation. On the other hand, *GTPBP3* overexpression slightly increased $\tau m^5U$ frequency from 16% to 27%, but the effect was limited compared with that of *MTO1* (Figure 3C). Although MTO1 and GTPBP3 work together, they have distinct roles in the $\tau m^5U$ modification of MELAS tRNA. In addition, the $\tau m^5U$ frequency of MELAS tRNA increased slightly from 16% to 28% in response to overexpression of *LARS2* CTD, although this effect was weak (Figure 3C). We also revealed by RNA-MS analysis that *MTO1* overexpression restored $\tau m^5s^2U$ frequency of the mutant mt-tRNA$^{Lys}$ in MERRF patient cells, and *TRMT61B* overexpression increased $m^1A58$ frequency in the same tRNA (Figure 6). $\tau m^5s^2U$ modification promotes accurate decoding of purine-ending codons (5). It is known that tRNAs with $m^1A58$ are enriched in polysome fraction in human cytoplasm (108), indicating that mt-tRNA$^{Lys}$ bearing both $\tau m^5s^2U$ and $m^1A58$ actively participates in protein synthesis. On the other hand, our group previously reported that $m^1A58$ of mt-tRNA$^{Lys}$ is constantly demethylated by ALKBH1 (109). This indicates that a heterogeneous population of differentially modified mt-tRNA$^{Lys}$, i.e. hypomodified mt-tRNA$^{Lys}$, may be involved in translational regulation in mitochondria.

*MTO1* overexpression slightly improved the aminoacylation rate of MELAS tRNA (Figure 4C). Because LARS2 leucylates two isoacceptors (20), mt-tRNA$^{Leu(UUR)}$ bearing $\tau m^5U$ and mt-tRNA$^{Leu(CUN)}$ without $\tau m^5U$, it is unlikely that LARS2 efficiently recognizes $\tau m^5U$-modified MELAS tRNA. Rather, MELAS tRNA might be transiently stabilized by MTO1 to facilitate recognition by LARS2. Some RNA-modifying enzymes can modulate RNA tertiary structures, which is known as an RNA chaperone function (110–113). MTO1 might work as an RNA chaperone to support mt-tRNA with pathogenic mutations for efficient aminoacylation.

In this study, *MTO1* overexpression fully restored $\tau m^5U$ frequency and partially increased the aminoacylation efficiency of MELAS tRNA, leading to the upregulation of

mitochondrial protein synthesis and respiratory activity in MELAS myoblasts (Figures 4D, E, and 5). The ECAR suggested that MELAS myoblasts had almost no respiration and relied solely on glycolysis for ATP production; however, *MTO1* overexpression activated MELAS myoblasts to initiate mitochondrial respiration to produce ATP. This finding clearly suggests that severe impairment of $\tau m^5U$ is a primary molecular pathogenesis of MELAS. Hence, restoration of $\tau m^5U$ may lead to potential treatments for MELAS. Although $\tau m^5U$ was almost fully restored by *MTO1* overexpression in MELAS myoblasts, mitochondrial function and respiratory activity were slightly improved but did not reach WT levels. This is because the steady-state level of MELAS tRNA remained low even if $\tau m^5U$ was fully introduced (Figure 4A and B). Our next target is thus to stabilize MELAS tRNA. We have three potential measures to achieve this: (i) searching for compounds or peptides that stabilize MELAS tRNA, (ii) inhibiting the degradation pathways of MELAS tRNA and (iii) stabilizing MELAS tRNA by introducing other tRNA modifications. We plan to continue our research efforts to develop more effective therapeutic measures for MELAS and related mitochondrial diseases.

## DATA AVAILABILITY

The data underlying this article are available in the article, its online supplementary material, and Source Data. All data supporting the findings in this study are available from the corresponding author upon reasonable request.

## SUPPLEMENTARY DATA

Supplementary Data are available at NAR Online.

## ACKNOWLEDGEMENTS

We are grateful to the members of the Suzuki laboratory, in particular, K. Miyauchi and Y. Sakaguchi, for technical support and insightful discussion. Radioisotope experiments were carried out with the support of the Isotope Science Center, University of Tokyo.

## FUNDING

Grant-in-Aid for Scientific Research from MEXT and JSPS [JSPS; 26113003, 26220205, 18H05272 to Ts.S., 26116003, 25660053 to A.N., 18H02094, 21H05280 to Ta.S.]; AMED [JP223fa627001 to Ts.S.]; JST [ERATO, JPMJER2002 to Ts.S.]; B.J.B. was supported by the Academy of Finland [314706]; Sigrid Juselius Foundation Senior Investigator Award. Funding for open access charge: Exploratory Research for Advanced Technology [ERATO, JPMJER2002] from the Japan Science and Technology Agency (JST).
*Conflict of interest statement.* None declared.

This paper is linked to: doi:10.1093/nar/gkad591.

## REFERENCES

1. Wallace,D.C. (2005) A mitochondrial paradigm of metabolic and degenerative diseases, aging, and cancer: a dawn for evolutionary medicine. *Annu. Rev. Genet.*, **39**, 359–407.
2. Rackham,O. and Filipovska,A. (2022) Organization and expression of the mammalian mitochondrial genome. *Nat. Rev. Genet.*, **23**, 606–623.
3. Anderson,S., Bankier,A.T., Barrell,B.G., de Bruijn,M.H., Coulson,A.R., Drouin,J., Eperon,I.C., Nierlich,D.P., Roe,B.A., Sanger,F. *et al.* (1981) Sequence and organization of the human mitochondrial genome. *Nature*, **290**, 457–465.
4. Hallberg,B.M. and Larsson,N.G. (2014) Making proteins in the powerhouse. *Cell Metab.*, **20**, 226–240.
5. Suzuki,T., Nagao,A. and Suzuki,T. (2011) Human mitochondrial tRNAs: biogenesis, function, structural aspects, and diseases. *Annu. Rev. Genet.*, **45**, 299–329.
6. Ayyub,S.A., Gao,F., Lightowlers,R.N. and Chrzanowska-Lightowlers,Z.M. (2020) Rescuing stalled mammalian mitoribosomes - what can we learn from bacteria?*J. Cell Sci.*, **133**, jcs231811.
7. Suomalainen,A. and Battersby,B.J. (2018) Mitochondrial diseases: the contribution of organelle stress responses to pathology. *Nat. Rev. Mol. Cell Biol.*, **19**, 77–92.
8. Gorman,G.S., Chinnery,P.F., DiMauro,S., Hirano,M., Koga,Y., McFarland,R., Suomalainen,A., Thorburn,D.R., Zeviani,M. and Turnbull,D.M. (2016) Mitochondrial diseases. *Nat. Rev. Dis. Primers*, **2**, 16080.
9. Lake,N.J., Compton,A.G., Rahman,S. and Thorburn,D.R. (2016) Leigh syndrome: one disorder, more than 75 monogenic causes. *Ann. Neurol.*, **79**, 190–203.
10. Goto,Y. (2000) Mitochondrial encephalomyopathy. *Neuropathology*, **20**(Suppl), S82–S84.
11. Lott,M.T., Leipzig,J.N., Derbeneva,O., Xie,H.M., Chalkia,D., Sarmady,M., Procaccio,V. and Wallace,D.C. (2013) mtDNA variation and analysis using mitomap and mitomaster. *Curr. Protoc. Bioinformatics*, **44**, 1.23.1–1.23.26.
12. Ruiz-Pesini,E., Lott,M.T., Procaccio,V., Poole,J.C., Brandon,M.C., Mishmar,D., Yi,C., Kreuziger,J., Baldi,P. and Wallace,D.C. (2007) An enhanced MITOMAP with a global mtDNA mutational phylogeny. *Nucleic Acids Res.*, **35**, D823–D828.
13. Pavlakis,S.G., Phillips,P.C., DiMauro,S., De Vivo,D.C. and Rowland,L.P. (1984) Mitochondrial myopathy, encephalopathy, lactic acidosis, and strokelike episodes: a distinctive clinical syndrome. *Ann. Neurol.*, **16**, 481–488.
14. Fukuhara,N., Tokiguchi,S., Shirakawa,K. and Tsubaki,T. (1980) Myoclonus epilepsy associated with ragged-red fibres (mitochondrial abnormalities): disease entity or a syndrome? Light-and electron-microscopic studies of two cases and review of literature. *J. Neurol. Sci.*, **47**, 117–133.
15. Goto,Y., Nonaka,I. and Horai,S. (1990) A mutation in the tRNA(Leu)(UUR) gene associated with the MELAS subgroup of mitochondrial encephalomyopathies. *Nature*, **348**, 651–653.
16. Goto,Y., Nonaka,I. and Horai,S. (1991) A new mtDNA mutation associated with mitochondrial myopathy, encephalopathy, lactic acidosis and stroke-like episodes (MELAS). *Biochim. Biophys. Acta*, **1097**, 238–240.
17. Kobayashi,Y., Momoi,M.Y., Tominaga,K., Momoi,T., Nihei,K., Yanagisawa,M., Kagawa,Y. and Ohta,S. (1990) A point mutation in the mitochondrial tRNA(Leu)(UUR) gene in MELAS (mitochondrial myopathy, encephalopathy, lactic acidosis and stroke-like episodes). *Biochem. Biophys. Res. Commun.*, **173**, 816–822.
18. Shoffner,J.M., Lott,M.T., Lezza,A.M., Seibel,P., Ballinger,S.W. and Wallace,D.C. (1990) Myoclonic epilepsy and ragged-red fiber disease (MERRF) is associated with a mitochondrial DNA tRNA(Lys) mutation. *Cell*, **61**, 931–937.
19. Sohm,B., Frugier,M., Brule,H., Olszak,K., Przykorska,A. and Florentz,C. (2003) Towards understanding human mitochondrial leucine aminoacylation identity. *J. Mol. Biol.*, **328**, 995–1010.
20. Sohm,B., Sissler,M., Park,H., King,M.P. and Florentz,C. (2004) Recognition of human mitochondrial tRNALeu(UUR) by its cognate leucyl-tRNA synthetase. *J. Mol. Biol.*, **339**, 17–29.
21. Yasukawa,T., Suzuki,T., Suzuki,T., Ueda,T., Ohta,S. and Watanabe,K. (2000) Modification defect at anticodon wobble nucleotide of mitochondrial tRNAs(Leu)(UUR) with pathogenic mutations of mitochondrial myopathy, encephalopathy, lactic acidosis, and stroke-like episodes. *J. Biol. Chem.*, **275**, 4251–4257.

22. Hess,J.F., Parisi,M.A., Bennett,J.L. and Clayton,D.A. (1991) Impairment of mitochondrial transcription termination by a point mutation associated with the MELAS subgroup of mitochondrial encephalomyopathies. *Nature*, **351**, 236–239.
23. Levinger,L., Oestreich,I., Florentz,C. and Morl,M. (2004) A pathogenesis-associated mutation in human mitochondrial tRNALeu(UUR) leads to reduced 3'-end processing and CCA addition. *J. Mol. Biol.*, **337**, 535–544.
24. Wittenhagen,L.M. and Kelley,S.O. (2002) Dimerization of a pathogenic human mitochondrial tRNA. *Nat. Struct. Biol.*, **9**, 586–590.
25. Borner,G.V., Zeviani,M., Tiranti,V., Carrara,F., Hoffmann,S., Gerbitz,K.D., Lochmuller,H., Pongratz,D., Klopstock,T., Melberg,A. *et al.* (2000) Decreased aminoacylation of mutant tRNAs in MELAS but not in MERRF patients. *Hum. Mol. Genet.*, **9**, 467–475.
26. Chomyn,A., Enriquez,J.A., Micol,V., Fernandez-Silva,P. and Attardi,G. (2000) The mitochondrial myopathy, encephalopathy, lactic acidosis, and stroke-like episode syndrome-associated human mitochondrial tRNALeu(UUR) mutation causes aminoacylation deficiency and concomitant reduced association of mRNA with ribosomes. *J. Biol. Chem.*, **275**, 19198–19209.
27. Park,H., Davidson,E. and King,M.P. (2003) The pathogenic A3243G mutation in human mitochondrial tRNALeu(UUR) decreases the efficiency of aminoacylation. *Biochemistry*, **42**, 958–964.
28. Fornuskova,D., Brantova,O., Tesarova,M., Stiburek,L., Honzik,T., Wenchich,L., Tietzeova,E., Hansikova,H. and Zeman,J. (2008) The impact of mitochondrial tRNA mutations on the amount of ATP synthase differs in the brain compared to other tissues. *Biochim. Biophys. Acta*, **1782**, 317–325.
29. Sasarman,F., Antonicka,H. and Shoubridge,E.A. (2008) The A3243G tRNALeu(UUR) MELAS mutation causes amino acid misincorporation and a combined respiratory chain assembly defect partially suppressed by overexpression of EFTu and EFG2. *Hum. Mol. Genet.*, **17**, 3697–3707.
30. King,M.P., Koga,Y., Davidson,M. and Schon,E.A. (1992) Defects in mitochondrial protein synthesis and respiratory chain activity segregate with the tRNA(Leu(UUR)) mutation associated with mitochondrial myopathy, encephalopathy, lactic acidosis, and strokelike episodes. *Mol. Cell. Biol.*, **12**, 480–490.
31. James,A.M., Wei,Y.H., Pang,C.Y. and Murphy,M.P. (1996) Altered mitochondrial function in fibroblasts containing MELAS or MERRF mitochondrial DNA mutations. *Biochem. J.*, **318**, 401–407.
32. Dunbar,D.R., Moonie,P.A., Zeviani,M. and Holt,I.J. (1996) Complex i deficiency is associated with 3243G:c mitochondrial DNA in osteosarcoma cell cybrids. *Hum. Mol. Genet.*, **5**, 123–129.
33. Kirino,Y., Goto,Y., Campos,Y., Arenas,J. and Suzuki,T. (2005) Specific correlation between the wobble modification deficiency in mutant tRNAs and the clinical features of a human mitochondrial disease. *Proc. Natl. Acad. Sci. U.S.A.*, **102**, 7127–7132.
34. Asano,K., Suzuki,T., Saito,A., Wei,F.Y., Ikeuchi,Y., Numata,T., Tanaka,R., Yamane,Y., Yamamoto,T., Goto,T. *et al.* (2018) Metabolic and chemical regulation of tRNA modification associated with taurine deficiency and human disease. *Nucleic Acids Res.*, **46**, 1565–1583.
35. Suzuki,T., Suzuki,T., Wada,T., Saigo,K. and Watanabe,K. (2002) Taurine as a constituent of mitochondrial tRNAs: new insights into the functions of taurine and human mitochondrial diseases. *EMBO J.*, **21**, 6581–6589.
36. Suzuki,T. and Suzuki,T. (2014) A complete landscape of post-transcriptional modifications in mammalian mitochondrial tRNAs. *Nucleic Acids Res.*, **42**, 7346–7357.
37. Kirino,Y., Yasukawa,T., Ohta,S., Akira,S., Ishihara,K., Watanabe,K. and Suzuki,T. (2004) Codon-specific translational defect caused by a wobble modification deficiency in mutant tRNA from a human mitochondrial disease. *Proc. Natl. Acad. Sci. U.S.A.*, **101**, 15070–15075.
38. Kurata,S., Weixlbaumer,A., Ohtsuki,T., Shimazaki,T., Wada,T., Kirino,Y., Takai,K., Watanabe,K., Ramakrishnan,V. and Suzuki,T. (2008) Modified uridines with C5-methylene substituents at the first position of the tRNA anticodon stabilize U.G wobble pairing during decoding. *J. Biol. Chem.*, **283**, 18801–18811.
39. Morscher,R.J., Ducker,G.S., Li,S.H., Mayer,J.A., Gitai,Z., Sperl,W. and Rabinowitz,J.D. (2018) Mitochondrial translation requires folate-dependent tRNA methylation. *Nature*, **554**, 128–132.
40. Hayashi,J., Ohta,S., Takai,D., Miyabayashi,S., Sakuta,R., Goto,Y. and Nonaka,I. (1993) Accumulation of mtDNA with a mutation at position 3271 in tRNA(Leu)(UUR) gene introduced from a MELAS patient to hela cells lacking mtDNA results in progressive inhibition of mitochondrial respiratory function. *Biochem. Biophys. Res. Commun.*, **197**, 1049–1055.
41. Koga,Y., Nonaka,I., Kobayashi,M., Tojyo,M. and Nihei,K. (1988) Findings in muscle in complex i (NADH coenzyme q reductase) deficiency. *Ann. Neurol.*, **24**, 749–756.
42. Goto,Y., Horai,S., Matsuoka,T., Koga,Y., Nihei,K., Kobayashi,M. and Nonaka,I. (1992) Mitochondrial myopathy, encephalopathy, lactic acidosis, and stroke-like episodes (MELAS): a correlative study of the clinical features and mitochondrial DNA mutation. *Neurology*, **42**, 545–550.
43. Yasukawa,T., Suzuki,T., Ishii,N., Ohta,S. and Watanabe,K. (2001) Wobble modification defect in tRNA disturbs codon-anticodon interaction in a mitochondrial disease. *EMBO J.*, **20**, 4794–4802.
44. Yasukawa,T., Suzuki,T., Ishii,N., Ueda,T., Ohta,S. and Watanabe,K. (2000) Defect in modification at the anticodon wobble nucleotide of mitochondrial tRNA(Lys) with the MERRF encephalomyopathy pathogenic mutation. *FEBS Lett.*, **467**, 175–178.
45. Yasukawa,T., Kirino,Y., Ishii,N., Holt,I.J., Jacobs,H.T., Makifuchi,T., Fukuhara,N., Ohta,S., Suzuki,T. and Watanabe,K. (2005) Wobble modification deficiency in mutant tRNAs in patients with mitochondrial diseases. *FEBS Lett.*, **579**, 2948–2952.
46. Boulet,L., Karpati,G. and Shoubridge,E.A. (1992) Distribution and threshold expression of the tRNA(Lys) mutation in skeletal muscle of patients with myoclonic epilepsy and ragged-red fibers (MERRF). *Am. J. Hum. Genet.*, **51**, 1187–1200.
47. Richter,U., Evans,M.E., Clark,W.C., Marttinen,P., Shoubridge,E.A., Suomalainen,A., Wredenberg,A., Wedell,A., Pan,T. and Battersby,B.J. (2018) RNA modification landscape of the human mitochondrial tRNA(Lys) regulates protein synthesis. *Nat. Commun.*, **9**, 3966.
48. Kopajtich,R., Nicholls,T.J., Rorbach,J., Metodiev,M.D., Freisinger,P., Mandel,H., Vanlander,A., Ghezzi,D., Carrozzo,R., Taylor,R.W. *et al.* (2014) Mutations in GTPBP3 cause a mitochondrial translation defect associated with hypertrophic cardiomyopathy, lactic acidosis, and encephalopathy. *Am. J. Hum. Genet.*, **95**, 708–720.
49. Baruffini,E., Dallabona,C., Invernizzi,F., Yarham,J.W., Melchionda,L., Blakely,E.L., Lamantea,E., Donnini,C., Santra,S., Vijayaraghavan,S. *et al.* (2013) MTO1 mutations are associated with hypertrophic cardiomyopathy and lactic acidosis and cause respiratory chain deficiency in humans and yeast. *Hum. Mutat.*, **34**, 1501–1509.
50. Ghezzi,D., Baruffini,E., Haack,T.B., Invernizzi,F., Melchionda,L., Dallabona,C., Strom,T.M., Parini,R., Burlina,A.B., Meitinger,T. *et al.* (2012) Mutations of the mitochondrial-tRNA modifier MTO1 cause hypertrophic cardiomyopathy and lactic acidosis. *Am. J. Hum. Genet.*, **90**, 1079–1087.
51. Fakruddin,M., Wei,F.Y., Suzuki,T., Asano,K., Kaieda,T., Omori,A., Izumi,R., Fujimura,A., Kaitsuka,T., Miyata,K. *et al.* (2018) Defective mitochondrial tRNA taurine modification activates global proteostress and leads to mitochondrial disease. *Cell Rep.*, **22**, 482–496.
52. Viscomi,C. and Zeviani,M. (2020) Strategies for fighting mitochondrial diseases. *J. Intern. Med.*, **287**, 665–684.
53. Silva-Pinheiro,P. and Minczuk,M. (2022) The potential of mitochondrial genome engineering. *Nat. Rev. Genet.*, **23**, 199–214.
54. Gammage,P.A., Rorbach,J., Vincent,A.I., Rebar,E.J. and Minczuk,M. (2014) Mitochondrially targeted ZFNs for selective degradation of pathogenic mitochondrial genomes bearing large-scale deletions or point mutations. *EMBO Mol. Med.*, **6**, 458–466.
55. Bacman,S.R., Williams,S.L., Pinto,M., Peralta,S. and Moraes,C.T. (2013) Specific elimination of mutant mitochondrial genomes in patient-derived cells by mitoTALENs. *Nat. Med.*, **19**, 1111–1113.
56. Yang,Y., Wu,H., Kang,X., Liang,Y., Lan,T., Li,T., Tan,T., Peng,J., Zhang,Q., An,G. *et al.* (2018) Targeted elimination of mutant

mitochondrial DNA in MELAS-iPSCs by mitoTALENs. *Protein Cell*, **9**, 283–297.
57. Park,H., Davidson,E. and King,M.P. (2008) Overexpressed mitochondrial leucyl-tRNA synthetase suppresses the A3243G mutation in the mitochondrial tRNA(Leu(UUR)) gene. *RNA*, **14**, 2407–2416.
58. Li,R. and Guan,M.X. (2010) Human mitochondrial leucyl-tRNA synthetase corrects mitochondrial dysfunctions due to the tRNALeu(UUR) A3243G mutation, associated with mitochondrial encephalomyopathy, lactic acidosis, and stroke-like symptoms and diabetes. *Mol. Cell. Biol.*, **30**, 2147–2154.
59. Hornig-Do,H.T., Montanari,A., Rozanska,A., Tuppen,H.A., Almalki,A.A., Abg-Kamaludin,D.P., Frontali,L., Francisci,S., Lightowlers,R.N. and Chrzanowska-Lightowlers,Z.M. (2014) Human mitochondrial leucyl tRNA synthetase can suppress non cognate pathogenic mt-tRNA mutations. *EMBO Mol. Med.*, **6**, 183–193.
60. Perli,E., Giordano,C., Pisano,A., Montanari,A., Campese,A.F., Reyes,A., Ghezzi,D., Nasca,A., Tuppen,H.A., Orlandi,M. *et al.* (2014) The isolated carboxy-terminal domain of human mitochondrial leucyl-tRNA synthetase rescues the pathological phenotype of mitochondrial tRNA mutations in human cells. *EMBO Mol. Med.*, **6**, 169–182.
61. Perli,E., Fiorillo,A., Giordano,C., Pisano,A., Montanari,A., Grazioli,P., Campese,A.F., Di Micco,P., Tuppen,H.A., Genovese,I. *et al.* (2016) Short peptides from leucyl-tRNA synthetase rescue disease-causing mitochondrial tRNA point mutations. *Hum. Mol. Genet.*, **25**, 903–915.
62. Perli,E., Pisano,A., Pignataro,M.G., Campese,A.F., Pelullo,M., Genovese,I., de Turris,V., Ghelli,A.M., Cerbelli,B., Giordano,C. *et al.* (2020) Exogenous peptides are able to penetrate human cell and mitochondrial membranes, stabilize mitochondrial tRNA structures, and rescue severe mitochondrial defects. *FASEB J.*, **34**, 7675–7686.
63. Chujo,T. and Suzuki,T. (2012) Trmt61B is a methyltransferase responsible for 1-methyladenosine at position 58 of human mitochondrial tRNAs. *RNA*, **18**, 2269–2276.
64. Rikimaru,M., Ohsawa,Y., Wolf,A.M., Nishimaki,K., Ichimiya,H., Kamimura,N., Nishimatsu,S., Ohta,S. and Sunada,Y. (2012) Taurine ameliorates impaired the mitochondrial function and prevents stroke-like episodes in patients with MELAS. *Intern. Med.*, **51**, 3351–3357.
65. Ohsawa,Y., Hagiwara,H., Nishimatsu,S.I., Hirakawa,A., Kamimura,N., Ohtsubo,H., Fukai,Y., Murakami,T., Koga,Y., Goto,Y.I. *et al.* (2019) Taurine supplementation for prevention of stroke-like episodes in MELAS: a multicentre, open-label, 52-week phase III trial. *J. Neurol. Neurosurg. Psychiatry*, **90**, 529–536.
66. Okegawa,Y. and Motohashi,K. (2015) Evaluation of seamless ligation cloning extract preparation methods from an escherichia coli laboratory strain. *Anal. Biochem.*, **486**, 51–53.
67. Dull,T., Zufferey,R., Kelly,M., Mandel,R.J., Nguyen,M., Trono,D. and Naldini,L. (1998) A third-generation lentivirus vector with a conditional packaging system. *J. Virol.*, **72**, 8463–8471.
68. Tiscornia,G., Singer,O. and Verma,I.M. (2006) Production and purification of lentiviral vectors. *Nat. Protoc.*, **1**, 241–245.
69. Campeau,E., Ruhl,V.E., Rodier,F., Smith,C.L., Rahmberg,B.L., Fuss,J.O., Campisi,J., Yaswen,P., Cooper,P.K. and Kaufman,P.D. (2009) A versatile viral system for expression and depletion of proteins in mammalian cells. *PLoS One*, **4**, e6529.
70. Wong,L.J. and Boles,R.G. (2005) Mitochondrial DNA analysis in clinical laboratory diagnostics. *Clin. Chim. Acta*, **354**, 1–20.
71. Miyauchi,K., Ohara,T. and Suzuki,T. (2007) Automated parallel isolation of multiple species of non-coding RNAs by the reciprocal circulating chromatography method. *Nucleic Acids Res.*, **35**, e24.
72. Suzuki,T., Ikeuchi,Y., Noma,A., Suzuki,T. and Sakaguchi,Y. (2007) Mass spectrometric identification and characterization of RNA-modifying enzymes. *Methods Enzymol.*, **425**, 211–229.
73. Suzuki,T., Yashiro,Y., Kikuchi,I., Ishigami,Y., Saito,H., Matsuzawa,I., Okada,S., Mito,M., Iwasaki,S., Ma,D. *et al.* (2020) Complete chemical structures of human mitochondrial tRNAs. *Nat. Commun.*, **11**, 4269.
74. Ohira,T., Minowa,K., Sugiyama,K., Yamashita,S., Sakaguchi,Y., Miyauchi,K., Noguchi,R., Kaneko,A., Orita,I., Fukui,T. *et al.* (2022) Reversible RNA phosphorylation stabilizes tRNA for cellular thermotolerance. *Nature*, **605**, 372–379.
75. Suzuki,T., Suzuki,T., Ueda,T. and Watanabe,K. (1999) High sensitive analysis of modified nucleosides by LC/MS using ESI/Iontrap mass spectrometry. *J. Mass Spectrom. Soc. Jpn.*, **46**, 168–176.
76. Varshney,U., Lee,C.P. and RajBhandary,U.L. (1991) Direct analysis of aminoacylation levels of tRNAs in vivo. Application to studying recognition of escherichia coli initiator tRNA mutants by glutaminyl-tRNA synthetase. *J. Biol. Chem.*, **266**, 24712–24718.
77. Nagao,A., Suzuki,T., Katoh,T., Sakaguchi,Y. and Suzuki,T. (2009) Biogenesis of glutaminyl-mt tRNAGln in human mitochondria. *Proc. Natl. Acad. Sci. U.S.A.*, **106**, 16209–16214.
78. Ho,N.W. and Gilham,P.T. (1967) The reversible chemical modification of uracil, thymine, and guanine nucleotides and the modification of the action of ribonuclease on ribonucleic acid. *Biochemistry*, **6**, 3632–3639.
79. Ho,N.W. and Gilham,P.T. (1971) Reaction of pseudouridine and inosine with N-cyclohexyl-N'-beta-(4-methylmorpholinium)ethylcarbodiimide. *Biochemistry*, **10**, 3651–3657.
80. Ofengand,J., Del Campo,M. and Kaya,Y. (2001) Mapping pseudouridines in RNA molecules. *Methods*, **25**, 365–373.
81. Karijolich,J., Yi,C. and Yu,Y.T. (2015) Transcriptome-wide dynamics of RNA pseudouridylation. *Nat. Rev. Mol. Cell Biol.*, **16**, 581–585.
82. Suzuki,T. (2021) The expanding world of tRNA modifications and their disease relevance. *Nat. Rev. Mol. Cell Biol.*, **22**, 375–392.
83. Rak,R., Polonsky,M., Eizenberg-Magar,I., Mo,Y., Sakaguchi,Y., Mizrahi,O., Nachshon,A., Reich-Zeliger,S., Stern-Ginossar,N., Dahan,O. *et al.* (2021) Dynamic changes in tRNA modifications and abundance during t cell activation. *Proc. Natl. Acad. Sci. U.S.A.*, **118**, e2106556118.
84. Rossello-Tortella,M., Llinas-Arias,P., Sakaguchi,Y., Miyauchi,K., Davalos,V., Setien,F., Calleja-Cervantes,M.E., Pineyro,D., Martinez-Gomez,J., Guil,S. *et al.* (2020) Epigenetic loss of the transfer RNA-modifying enzyme TYW2 induces ribosome frameshifts in colon cancer. *Proc. Natl. Acad. Sci. U.S.A.*, **117**, 20785–20793.
85. Roundtree,I.A., Evans,M.E., Pan,T. and He,C. (2017) Dynamic RNA modifications in gene expression regulation. *Cell*, **169**, 1187–1200.
86. Hanson,G. and Coller,J. (2018) Codon optimality, bias and usage in translation and mRNA decay. *Nat. Rev. Mol. Cell Biol.*, **19**, 20–30.
87. Pechmann,S. and Frydman,J. (2013) Evolutionary conservation of codon optimality reveals hidden signatures of cotranslational folding. *Nat. Struct. Mol. Biol.*, **20**, 237–243.
88. Nedialkova,D.D. and Leidel,S.A. (2015) Optimization of codon translation rates via tRNA modifications maintains proteome integrity. *Cell*, **161**, 1606–1618.
89. Chujo,T. and Tomizawa,K. (2021) Human transfer RNA modopathies: diseases caused by aberrations in transfer RNA modifications. *FEBS J.*, **288**, 7096–7122.
90. Torres,A.G., Batlle,E. and Ribas de Pouplana,L. (2014) Role of tRNA modifications in human diseases. *Trends Mol. Med.*, **20**, 306–314.
91. Ross,R.L., Cao,X. and Limbach,P.A. (2017) Mapping post-transcriptional modifications onto transfer ribonucleic acid sequences by liquid chromatography tandem mass spectrometry. *Biomolecules*, **7**, 21.
92. Wolff,P., Villette,C., Zumsteg,J., Heintz,D., Antoine,L., Chane-Woon-Ming,B., Droogmans,L., Grosjean,H. and Westhof,E. (2020) Comparative patterns of modified nucleotides in individual tRNA species from a mesophilic and two thermophilic archaea. *RNA*, **26**, 1957–1975.
93. Pomerantz,S.C. and McCloskey,J.A. (1990) Analysis of RNA hydrolyzates by liquid chromatography-mass spectrometry. *Methods Enzymol.*, **193**, 796–824.
94. Su,D., Chan,C.T., Gu,C., Lim,K.S., Chionh,Y.H., McBee,M.E., Russell,B.S., Babu,I.R., Begley,T.J. and Dedon,P.C. (2014) Quantitative analysis of ribonucleoside modifications in tRNA by HPLC-coupled mass spectrometry. *Nat. Protoc.*, **9**, 828–841.
95. Sakaguchi,Y., Miyauchi,K., Kang,B.I. and Suzuki,T. (2015) Nucleoside analysis by hydrophilic interaction liquid

chromatography coupled with mass spectrometry. *Methods Enzymol.*, **560**, 19–28.
96. Li,X., Xiong,X. and Yi,C. (2016) Epitranscriptome sequencing technologies: decoding RNA modifications. *Nat. Methods*, **14**, 23–31.
97. Kimura,S., Dedon,P.C. and Waldor,M.K. (2020) Comparative tRNA sequencing and RNA mass spectrometry for surveying tRNA modifications. *Nat. Chem. Biol.*, **16**, 964–972.
98. Wang,J., Toffano-Nioche,C., Lorieux,F., Gautheret,D. and Lehmann,J. (2021) Accurate characterization of escherichia coli tRNA modifications with a simple method of deep-sequencing library preparation. *RNA Biol*, **18**, 33–46.
99. Helm,M. and Motorin,Y. (2017) Detecting RNA modifications in the epitranscriptome: predict and validate. *Nat. Rev. Genet.*, **18**, 275–291.
100. Suzuki,T. (2005) In: Grosjean,H. (ed). *Fine-Tuning of RNA Functions by Modification and Editing*. Springer-Verlag Berlin and Heidelberg GmbH & Co. KG, Vol. **12**, pp. 23–69.
101. Liu,C.L., Watson,A.M., Place,A.R. and Jagus,R. (2017) Taurine biosynthesis in a fish liver cell line (ZFL) adapted to a serum-free medium. *Mar Drugs*, **15**, 147.
102. Umeda,N., Suzuki,T., Yukawa,M., Ohya,Y., Shindo,H., Watanabe,K. and Suzuki,T. (2005) Mitochondria-specific RNA-modifying enzymes responsible for the biosynthesis of the wobble base in mitochondrial tRNAs. Implications for the molecular pathogenesis of human mitochondrial diseases. *J. Biol. Chem.*, **280**, 1613–1624.
103. Sakurai,M., Ohtsuki,T., Suzuki,T. and Watanabe,K. (2005) Unusual usage of wobble modifications in mitochondrial tRNAs of the nematode ascaris suum. *FEBS Lett.*, **579**, 2767–2772.
104. Bommisetti,P., Young,A. and Bandarian,V. (2022) Elucidation of the substrate of tRNA-modifying enzymes MnmEG leads to in vitro reconstitution of an evolutionarily conserved uridine hypermodification. *J. Biol. Chem.*, **298**, 102548.
105. Moukadiri,I., Prado,S., Piera,J., Velazquez-Campoy,A., Bjork,G.R. and Armengod,M.E. (2009) Evolutionarily conserved proteins MnmE and GidA catalyze the formation of two methyluridine derivatives at tRNA wobble positions. *Nucleic Acids Res.*, **37**, 7177–7193.
106. Urbonavicius,J., Skouloubris,S., Myllykallio,H. and Grosjean,H. (2005) Identification of a novel gene encoding a flavin-dependent tRNA:m5U methyltransferase in bacteria–evolutionary implications. *Nucleic Acids Res.*, **33**, 3955–3964.
107. Osawa,T., Ito,K., Inanaga,H., Nureki,O., Tomita,K. and Numata,T. (2009) Conserved cysteine residues of GidA are essential for biogenesis of 5-carboxymethylaminomethyluridine at tRNA anticodon. *Structure*, **17**, 713–724.
108. Liu,F., Clark,W., Luo,G., Wang,X., Fu,Y., Wei,J., Wang,X., Hao,Z., Dai,Q., Zheng,G. *et al.* (2016) ALKBH1-Mediated tRNA demethylation regulates translation. *Cell*, **167**, 816–828.
109. Kawarada,L., Suzuki,T., Ohira,T., Hirata,S., Miyauchi,K. and Suzuki,T. (2017) ALKBH1 is an RNA dioxygenase responsible for cytoplasmic and mitochondrial tRNA modifications. *Nucleic Acids Res.*, **45**, 7401–7415.
110. Ishitani,R., Yokoyama,S. and Nureki,O. (2008) Structure, dynamics, and function of RNA modification enzymes. *Curr. Opin. Struct. Biol.*, **18**, 330–339.
111. Keffer-Wilkes,L.C., Veerareddygari,G.R. and Kothe,U. (2016) RNA modification enzyme TruB is a tRNA chaperone. *Proc. Natl. Acad. Sci. U.S.A.*, **113**, 14306–14311.
112. Keffer-Wilkes,L.C., Soon,E.F. and Kothe,U. (2020) The methyltransferase TrmA facilitates tRNA folding through interaction with its RNA-binding domain. *Nucleic Acids Res.*, **48**, 7981–7990.
113. Kimura,S., Ikeuchi,Y., Kitahara,K., Sakaguchi,Y., Suzuki,T. and Suzuki,T. (2012) Base methylations in the double-stranded RNA by a fused methyltransferase bearing unwinding activity. *Nucleic Acids Res.*, **40**, 4071–4085.